Circulation Research
JOURNAL OF THE AMERICAN HEART ASSOCIATION

SAP97 and Dystrophin Macromolecular Complexes Determine Two Pools of Cardiac Sodium Channels $Na_V1.5$ in Cardiomyocytes

Séverine Petitprez, Anne-Flore Zmoos, Jakob Ogrodnik, Elise Balse, Nour Raad, Said El-Haou, Maxime Albesa, Philip Bittihn, Stefan Luther, Stephan E. Lehnart, Stéphane N. Hatem, Alain Coulombe and Hugues Abriel

Circulation Research 2011, 108:294-304: originally published online December 16, 2010
doi: 10.1161/CIRCRESAHA.110.228312
Circulation Research is published by the American Heart Association. 7272 Greenville Avenue, Dallas, TX 72514
 Print ISSN: 0009-7330. Online ISSN: 1524-4571

SAP97 and Dystrophin Macromolecular Complexes Determine Two Pools of Cardiac Sodium Channels $Na_v1.5$ in Cardiomyocytes

Séverine Petitprez,* Anne-Flore Zmoos,* Jakob Ogrodnik, Elise Balse, Nour Raad, Said El-Haou, Maxime Albesa, Philip Bittihn, Stefan Luther, Stephan E. Lehnart, Stéphane N. Hatem, Alain Coulombe, Hugues Abriel

Rationale: **The cardiac sodium channel $Na_v1.5$ plays a key role in excitability and conduction. The 3 last residues of $Na_v1.5$ (Ser-Ile-Val) constitute a PDZ-domain binding motif that interacts with the syntrophin–dystrophin complex. As dystrophin is absent at the intercalated discs, $Na_v1.5$ could potentially interact with other, yet unknown, proteins at this site.**

Objective: **The aim of this study was to determine whether $Na_v1.5$ is part of distinct regulatory complexes at lateral membranes and intercalated discs.**

Methods and Results: **Immunostaining experiments demonstrated that $Na_v1.5$ localizes at lateral membranes of cardiomyocytes with dystrophin and syntrophin. Optical measurements on isolated dystrophin-deficient mdx hearts revealed significantly reduced conduction velocity, accompanied by strong reduction of $Na_v1.5$ at lateral membranes of mdx cardiomyocytes. Pull-down experiments revealed that the MAGUK protein SAP97 also interacts with the SIV motif of $Na_v1.5$, an interaction specific for SAP97 as no pull-down could be detected with other cardiac MAGUK proteins (PSD95 or ZO-1). Furthermore, immunostainings showed that $Na_v1.5$ and SAP97 are both localized at intercalated discs. Silencing of SAP97 expression in HEK293 and rat cardiomyocytes resulted in reduced sodium current (I_{Na}) measured by patch-clamp. The I_{Na} generated by $Na_v1.5$ channels lacking the SIV motif was also reduced. Finally, surface expression of $Na_v1.5$ was decreased in silenced cells, as well as in cells transfected with SIV-truncated channels.**

Conclusions: **These data support a model with at least 2 coexisting pools of $Na_v1.5$ channels in cardiomyocytes: one targeted at lateral membranes by the syntrophin-dystrophin complex, and one at intercalated discs by SAP97. (*Circ Res*. 2011;108:294-304.)**

Key Words: sodium channel ■ $Na_v1.5$ ■ MAGUK proteins ■ SAP97 ■ dystrophin

The cardiac sodium channel $Na_v1.5$ initiates the cardiac action potential, thus playing a key role in cardiac excitability and impulse propagation. The physiological importance of this channel is illustrated by numerous cardiac pathologies caused by hundreds of mutations identified in *SCN5A*, the gene encoding $Na_v1.5$.[1] The $Na_v1.5$ channel is composed of one 220-kDa α-subunit that constitutes a functional channel, and 30-kDa β-subunits. In addition to these accessory β-subunits, several proteins have been shown to regulate and interact with $Na_v1.5$.[1,2] In most cases, the physiological relevance of these interactions is poorly understood, mainly because of a lack of appropriate animal models. Many of the interacting proteins bind to the C terminus of $Na_v1.5$, where several protein–protein interaction motifs are located.[1,2] We have shown that the ubiquitin–protein ligase Nedd4-2 binds the PY motif of $Na_v1.5$ and reduces the sodium current (I_{Na}) in HEK293 cells by promoting its internalization.[3] We have also demonstrated that $Na_v1.5$ associates with the dystrophin–syntrophin multiprotein complex (DMC) in cardiac cells.[4] In dystrophin-deficient mice (mdx^{5cv}), I_{Na} and total $Na_v1.5$ protein expression are reduced. The association between $Na_v1.5$ and dystrophin occurs via

Original received October 6, 2009; resubmission received July 17, 2010; revised resubmission received December 3, 2010; accepted December 8, 2010. In November 2010, the average time from submission to first decision for all original research papers submitted to *Circulation Research* was 13.2 days.

From the Department of Clinical Research (S.P., A.-F.Z., J.O., M.A., H.A.), University of Bern, Switzerland; INSERM UMRS 956 (S.P., E.B., S.E.-H., S.N.H., A.C.), Université Pierre et Marie Curie-Paris 6, Paris, France; Max Planck Institute for Dynamics and Self-Organization (N.R., P.B., S.L.), Göttingen, Germany; Department of Cardiology & Pulmonology (N.R., S.E.L.), Heart Research Center Goettingen, University Medical Center Göttingen, Germany; Department of Biomedical Sciences (S.L.), Cornell University, Ithaca, NY; and Center for Biomedical Engineering and Technology (S.E.L.), University of Maryland Baltimore, Baltimore, MD.

*Both authors contributed equally to this work.

Correspondence to Dr Hugues Abriel, MD, PhD, University of Bern, Department of Clinical Research, Murtenstrasse, 35, 3010 Bern, Switzerland. E-mail Hugues.Abriel@dkf.unibe.ch

Circulation Research **is available at http://circres.ahajournals.org** **DOI: 10.1161/CIRCRESAHA.110.228312**

the syntrophin family of adaptor proteins, 3 of which are expressed in the heart.[4] The PDZ domain of syntrophin binds to the last 3 C-terminal residues of $Na_v1.5$ (Ser-Ile-Val, SIV), a PDZ-domain binding motif that mediates the interaction with dystrophin and other proteins of the DMC.[2] Interestingly, dystrophin has been shown to be absent from the intercalated discs of human[6] and rat[7] cardiac cells, suggesting that the $Na_v1.5$ channels present at these locations may interact with other regulatory or anchoring proteins.

Proteins of the membrane associated guanylate kinase (MAGUK) family are characterized by numerous protein–protein interaction domains, including PDZ domains.[8] They are involved in the function and localization of many ion channels in neurons and epithelial cells, mostly at cell to cell junctions, but little is known about their function in the heart.[9] SAP97 (synapse associated protein) and ZO-1 (zonula occludens) are the main MAGUK proteins expressed in cardiomyocytes.[9] PSD95 (postsynaptic density) is also expressed in the human heart, but not in the mouse heart.[9,10] SAP97 regulates the targeting and localization of cardiac potassium channels, such as Kir2.x[11] and $K_v1.5$ in myocytes.[10] El-Haou et al[12] recently demonstrated that SAP97 interacts with $K_v4.2$ and $K_v4.3$ channels via their PDZ-domain binding motif. They showed that suppression of SAP97 expression in rat myocytes decreases the $K_v4.x$-mediated current, whereas its overexpression increases it. In neurons, PSD95, which is closely related to SAP97, plays a role in clustering and anchoring ion channels to the postsynaptic plasma membrane.[13] Because PSD95 is also present in the human heart and SAP97 has been shown to interact with potassium channels in cardiac cells, we hypothesized that one of these cardiac MAGUK proteins may also associate with $Na_v1.5$.

In this study, we provide evidence for the coexistence of at least 2 pools of $Na_v1.5$ channels in cardiomyocytes, one located at the lateral membrane with the DMC, and the other localizing with SAP97 at the intercalated discs. In sections and isolated cardiomyocytes of dystrophin-deficient mice, we observed a drastic reduction of the pool of $Na_v1.5$ channels located at the lateral membrane. This loss could underlie the significant reduction of conduction velocity observed in these dystrophin-deficient hearts using optical measurements. Finally, we also found that the surface expression of $Na_v1.5$ in HEK293 cells is regulated by its interaction with SAP97.

Non-standard Abbreviations and Acronyms	
Cx	connexin
CV	conduction velocity
DMC	dystrophin multiprotein complex
MAGUK	membrane-associated guanylate kinase
PSD95	Postsynaptic density 95
SAP97	synapse-associated protein 97
shRNA	short hairpin RNA
WT	wild type
ZO	zonula occludens

Methods

An expanded Methods section is available in the Online Data Supplement at http://circres.ahajournals.org.

Cell Preparation, Transfection, and Infection

HEK293 and Sk-Hep cells were cultured as previously described.[3]

Silencing and Lentiviruses

HEK293 cells stably expressing $Na_v1.5$ were transfected using Lipofectamine (Invitrogen) as detailed in the Online Data Supplement. HEK293 cells were infected with VSV-G pseudo-typed lentiviruses.[14] Adult rat cardiomyocytes were transfected with silencing plasmids, as previously published.[12]

Transfection

For patch-clamp experiments, HEK293 cells were transiently transfected using calcium phosphate with the different constructs mentioned in the text. Details are given in the Online Data Supplement.

Protein Extraction, Pull-Down, and Western Blot

These procedures were performed as previously reported with HEK293 and Sk-Hep cells.[4] See Online Data Supplement for other tissues.

Biotinylation Assay

Transfected HEK293 cells were biotinylated as detailed in the Online Data Supplement. Biotinylated proteins were then analyzed by Western blot.

Immunohistochemistry of Rat and Mouse Ventricular Sections

Immunostainings were performed on heart cryosections as described in the Online Data Supplement.

Isolation and Immunocytochemistry of Mouse Ventricular Myocytes

See the Online Data Supplement for a detailed description.

Electrophysiology

Patch-clamp recordings were carried out in the whole-cell configuration at room temperature using solutions previously described.[4] See the Online Data Supplement for details.

Conduction Velocity Measurements on Isolated Mouse Hearts

Optical measurements of conduction velocity (CV) were performed on isolated wild-type and dystrophin-deficient mdx mouse hearts as described in detail in the Online Data Supplement.

Statistical Analysis

Data are represented as mean values±SEM, unless otherwise indicated.

Results

$Na_v1.5$ Is Localized With Dystrophin and Syntrophins Only at the Lateral Membrane

We recently demonstrated that $Na_v1.5$ associates with the DMC in cardiac cells.[4] We also observed that sodium current (I_{Na}) and $Na_v1.5$ protein expression is reduced in dystrophin-deficient (mdx^{5cv}) mice compared to wild type (WT).[4] To further study the importance of this multiprotein complex, we analyzed the distribution of $Na_v1.5$ channels, as well as that of dystrophin and syntrophin in rat ventricular sections (Figure 1A and 1B). Immunostaining experiments showed that $Na_v1.5$ is distributed along the entire membrane of rat cardiomyocytes (Figure 1A and 1B, left). In contrast, we

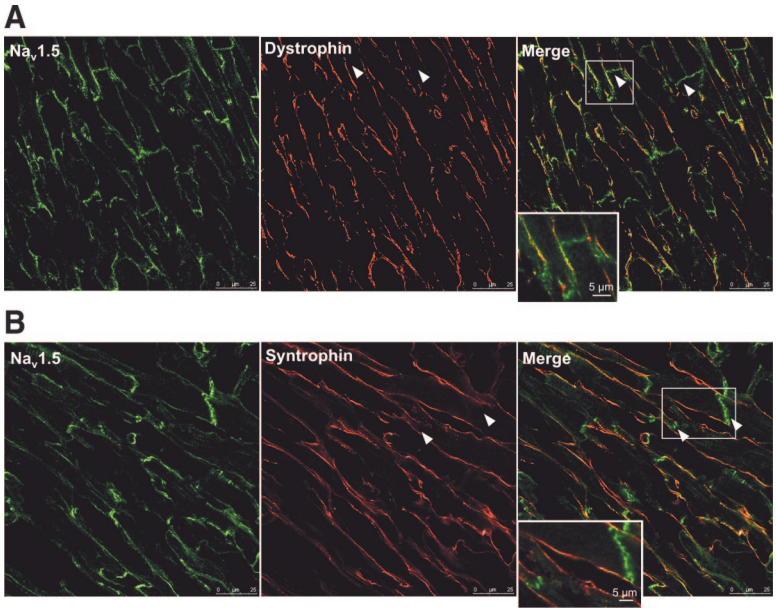

Figure 1. Localization of Na$_v$1.5, dystrophin and syntrophin in rat ventricular sections. A, Left,** Na$_v$1.5 **(green) is present both at the lateral membranes and the intercalated discs. **Middle,** Dystrophin **(red)** is only localized at the lateral membranes. **Right,** Merge of the 2 images showing close localization of Na$_v$1.5 and dystrophin at the lateral membranes. **White arrowheads** show the absence of dystrophin at the intercalated discs. **Inset,** Magnification of a portion of cell. **B, Left,** Na$_v$1.5 **(green)** is present both at the lateral membranes and the intercalated discs. **Middle,** syntrophin **(red)** is only at the lateral membranes. **Right,** Merge of the 2 images showing close localization of Na$_v$1.5 and syntrophin at the lateral membranes. The **white arrowheads** show the absence of syntrophin at the intercalated discs; inset: magnification of a portion of cell.

observed that Na$_v$1.5 and dystrophin are in the same membrane compartment exclusively at the lateral membrane (Figure 1A, right), and not at the intercalated discs, where dystrophin is absent (white arrowheads, Figure 1A, middle and right). Similar results were obtained using an antibody that recognized all syntrophin isoforms (Figure 1B). Syntrophins are similarly in close proximity to Na$_v$1.5 exclusively at the lateral membrane (Figure 1B, white arrowheads). In mouse ventricular sections, similar findings were obtained with Na$_v$1.5, dystrophin, and syntrophin (Online Figure I). These results suggest that Na$_v$1.5 could be part of at least 2 different protein complexes: with dystrophin at the lateral membrane and with another partner at the intercalated discs.

Na$_v$1.5 Is Decreased at the Lateral Membranes of Dystrophin-Deficient Myocytes

Immunohistochemistry experiments were performed using WT and mdx^{5cv} mouse ventricular sections (Figure 2A). A strong reduction of Na$_v$1.5 staining was observed at the lateral membrane of mdx^{5cv} mouse cardiomyocytes (Figure 2A, bottom) compared to WT mice (Figure 2A, top). Similarly, immunocytochemistry performed on isolated mouse cardiomyocytes confirmed that Na$_v$1.5 is distributed along the entire cell membrane in these cells, and that lateral Na$_v$1.5 staining in dystrophin-deficient cardiomyocytes is strongly reduced when compared to WT (Figure 2B). These results suggest that the decrease in Na$_v$1.5 protein and I_{Na} previously seen in dystrophin-deficient mice[4] is the consequence of a loss of Na$_v$1.5 channels at the lateral membrane of cardiomyocytes.

Impulse Propagation Is Significantly Slowed in Hearts of mdx Mice

Reduced I_{Na} and Na$_v$1.5 protein in dystrophin-deficient hearts may contribute to the previously observed prolongation of the QRS complex duration observed in ECG recordings of mdx^{5cv} mice.[4] To investigate whether conduction velocity (CV) is reduced in dystrophin-deficient hearts, we performed optical measurements in isolated Langendorff-perfused WT and mdx hearts stained with the fluorescent voltage-reporter dye Di-4-ANNEPS. Conduction spread of the paced (cycle length 100 ms) left ventricle free wall was recorded following equilibration and confirmation of physiological spontaneous heart rates (500 to 600/min, by volumetric ECG). Maximal CV occurred in the same direction in WT and mdx hearts along the longitudinal (apico-aortal) heart axis. Isochrone maps from WT hearts showed regular anisotropic conduction spread around a point-like pacing stimulus originating from the free LV wall center (Figure 3A, left). Accordingly, CV analysis by ellipsis fitting confirmed longitudinal and transversal velocities consistent with rapid ellipsoid conduction spread and physiological anisotropy (Figure 3A, right) (see online supplemental methods for detailed description). However, conduction spread of mdx hearts resulted in tighter isochrone maps indicating conduction slowing in all directions (Figure 3B, left). In agreement with this observation ellipsis fitting analysis confirmed slowing of conduction spread in the transversal axis resulting in reduced conduction velocities (Figure 3B, right). Figure 3C shows that in contrast to WT hearts, dystrophin-deficient hearts showed on average a reduction in transversal CV by 22.2% from 0.45±0.08 m/sec to 0.35±0.07 m/sec (WT n=5, mdx n=8; $P<0.05$) and in longitudinal CV by 12.7% from 0.71±0.14 m/sec to 0.62±0.11 m/sec (WT n=5, mdx n=8; P=NS).

Additionally, CV has been analyzed by a second method using averaged CV vectors along the apparent longitudinal and transversal heart axis (see online supplementary methods for detailed description). Figure 3D confirms that in contrast to WT hearts, dystrophin-deficient hearts showed a longitudinal 28.4% reduction in CV (WT n=5, mdx n=8; $P<0.005$). In addition, transversal CV was significantly reduced by 22.4% in mdx compared to WT hearts (WT n=5, mdx n=8; $P<0.05$; Figure 3D). The combined reduction of transversal and longitudinal CVs resulted in a 7.3% reduction in the anisotropic ratio (WT n=5, mdx n=8; P=NS; Figure 3D) when analyzed by averaged CV vectors and by 10.7%

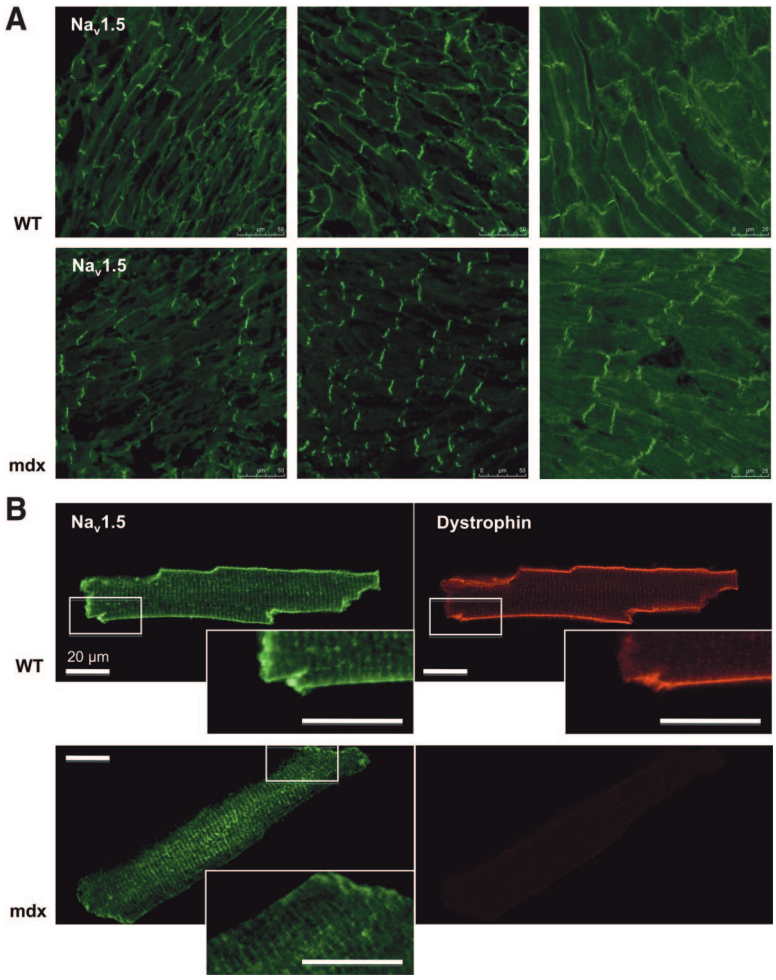

Figure 2. Loss of $Na_v1.5$ lateral membrane staining in dystrophin-deficient cardiomyocytes. A, $Na_v1.5$ **(green)** in WT **(top)** and mdx^{5cv} **(bottom)** ventricular sections. Note the loss of lateral membrane $Na_v1.5$ staining in the mdx^{5cv} sections; intercalated disc staining remains almost unaffected. **B,** Cardiomyocytes labeled for $Na_v1.5$ **(green, left)** and dystrophin **(red, right)**. Note the absence of dystrophin staining at the intercalated discs in WT cardiomyocytes (cf, **insets** with magnifications). Mdx cardiomyocytes were identified by the negative dystrophin staining **(bottom, right)**. In isolated mdx cardiomyocytes, $Na_v1.5$ staining was similarly markedly reduced at the lateral membrane.

when analyzed by the ellipsis fitting method (WT n=5, mdx n=8; *P*=NS; Figure 3C). Thus, under quasi-physiological conditions mimicking the resting mouse heart rate of 600/min the mdx left ventricle showed significantly slower excitation spread both in the longitudinal and transversal directions, confirming the slowed impulse propagation suggested by the widening of QRS complex. As distribution and expression of the main ventricular connexin, Cx43, is unaltered in mdx hearts (see Online Figure II and elsewhere[4]), this may suggest a selective role of $Na_v1.5$ channels located at the lateral membrane for impulse propagation in cardiac muscle.

The Carboxyl Terminus of $Na_v1.5$ Interacts With SAP97

To identify proteins that could specifically interact with the fractions of $Na_v1.5$ at the intercalated discs, we studied proteins of the MAGUK family. We performed pull-down experiments using GST-fusion proteins comprising the last 66 amino acids of the C terminus (C-ter) of $Na_v1.5$, as well as fusion proteins lacking the 3 last SIV residues (ΔSIV, Figure 4A). Western blot experiments performed using an anti-PSD95 family antibody, known to recognize several cardiac MAGUKs (Figure 4B, Online Figure III), revealed that $Na_v1.5$ C-ter WT precipitated proteins containing PDZ domains (2 bands at ≈140 kDa, the molecular weight of SAP97) from mouse ventricles and human atrium. This interaction is dependent on the PDZ-domain binding motif of $Na_v1.5$, as no protein was observed with the truncated construct. Similar results were obtained using a SAP97 specific antibody (Figure 4C, Online Figure III). The similarity between these 2 results (Figure 4B and 4C) suggests that SAP97 is the predominant MAGUK interacting with $Na_v1.5$. To assess if this interaction was specific for SAP97, we tested a specific PSD95 antibody (Figure 4D). No interaction was seen with either fusion protein ($Na_v1.5$ C-ter WT or ΔSIV). We also verified whether $Na_v1.5$ C terminus could interact with ZO-1, a cardiac MAGUK protein known to interact with connexins. We generated a fusion protein containing the last amino acids of connexin-45 (Cx45) (Figure 4A), which has previously been shown to bind ZO-1.[15] Pull-down experiments performed using SK-Hep cell lysates, which express ZO-1 endogenously, confirmed that Cx45 C-ter precipitated ZO-1, but that $Na_v1.5$ C-ter (Figure 4E) did not. Combined, these results support a specific interaction between the PDZ-domain binding motif of $Na_v1.5$ and SAP97 in mouse ventricles and human atria.

Localization of SAP97, $Na_v1.5$, Cx43, and Syntrophin in Rat Cardiomyocytes

To analyze the distribution of $Na_v1.5$ and SAP97 in native cardiac tissue, we performed immunostainings using $Na_v1.5$, SAP97 and Cx43 antibodies on rat heart sections. As present-

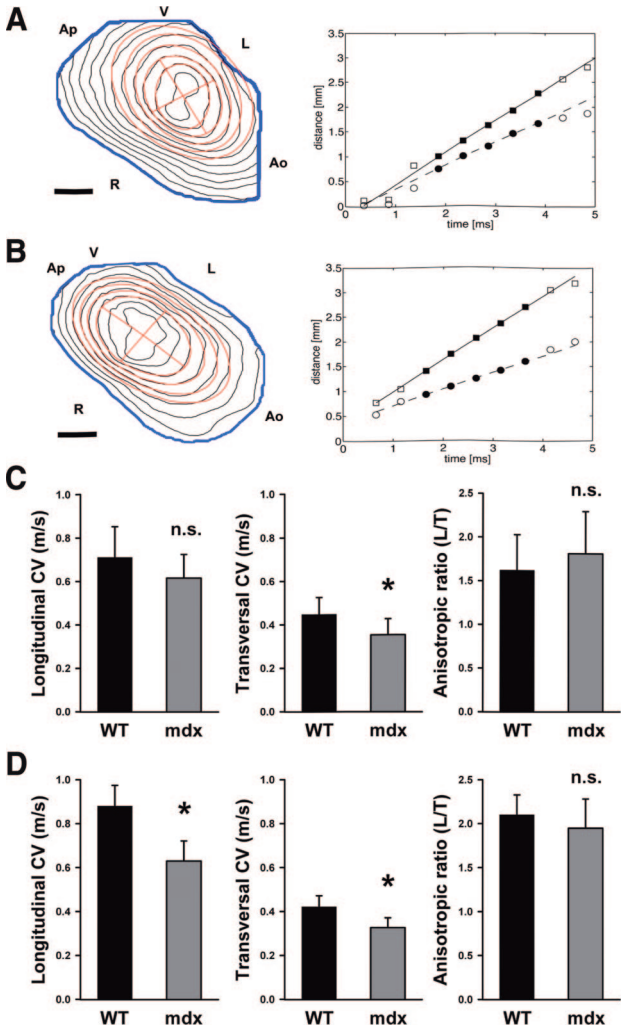

Figure 3. Left ventricle conduction slowing in mdx hearts. Paced activation of **(A, left)** representative WT heart characterized by averaged 0.5-ms contour isochrone map showing normal elliptic conduction spread and expected anisotropic behavior versus **(B, left)** mdx heart showing "crowding" of averaged 0.5-ms isochrone contours, indicating slowed activation of the LV substrate. **Bars,** 1 mm each. Ap indicates apex; L, left; R, right; Ao, aorta; point of pacing stimulus is located in the isochrone map center; V, peripheral position of pacing electrode with the electrode stimulation pulse occurring at the isochrone center. **A and B, Right,** Ellipsis fitting analysis of conduction velocity from the same WT and mdx hearts shown on left: **filled symbols** are determined by individual ellipsis fit indicated in **red color on left side**. Changes in CV in the mdx heart are indicated by a reduced slope in conduction spread by corresponding data points **(filled symbols)**; data points deviating from the linear trend attributable to proximity to pace site or organ borders were excluded from the analysis **(open symbols)**. **C,** Bar graphs summarizing average CV and anisotropic ratio from ellipsis fitting analysis. **D,** Bar graphs summarizing average CV and anisotropic ratio from averaged longitudinal and transversal vector analysis. Data in **C and D** are represented as means±SD. *$P<0.05$; ns, not significant as indicated.

ed in Figure 5A, SAP97 is predominantly expressed at the intercalated discs (Figure 5A, middle) where $Na_v1.5$ is also observed (white arrowheads, Figure 5A right). We also performed coimmunostainings of SAP97 and Cx43, showing that both proteins are located at the intercalated discs (white arrowheads, Figure 5B, right).

Silencing of SAP97 in HEK293 Cells, Cardiomyocytes, and $Na_v1.5$ Channels Lacking the SIV-Domain Reduces I_{Na}

The results presented in Figure 4 indicate that $Na_v1.5$ and SAP97 interact via their SIV-motif and PDZ domain, respectively. Electrophysiological studies were performed to characterize the role of this interaction. First, patch-clamp experiments using HEK293 cells transiently transfected with $Na_v1.5$ and SAP97 were carried out. Unexpectedly, expression of SAP97 did not modify I_{Na} (not shown). This result could be an indication that endogenous SAP97 is expressed at a saturating level in HEK293 cells. We subsequently reduced the expression of SAP97 using short hairpin (sh)RNA. When HEK293 cells expressing $Na_v1.5$ (HEK293-$Na_v1.5$) were transfected with SAP97 silencing plasmids, I_{Na} was reduced by 55±4% (Figure 6B). However, the transfection technique was not efficient enough to silence SAP97 expression in the majority of the cells. Therefore, we developed a lentivirus-based strategy to deliver shRNA. Western-blots performed with HEK293 cells infected with shRNA-containing lentiviruses revealed that SAP97 expression was drastically reduced (−83%, Figure 6A) when compared to nonsilenced cells infected with scrambled shRNA. In HEK293-$Na_v1.5$ cells silenced with lentiviruses, we observed a reduction of I_{Na} that was comparable to the results obtained when using the silencing plasmid (not shown). Next, we studied the consequence of silencing SAP97 on endogenous I_{Na} in rat atrial myocytes maintained in short term culture. This procedure has been previously shown to efficiently suppress endogenous cardiac SAP97.[12] After 3 to 4 days of culture, current recordings at -20 mV using green-fluorescent atrial myocytes (≈20% of the cells) revealed a much smaller I_{Na} in myocytes transfected with shSAP97 than those with scrambled shRNA (−66±8%, Figure 6C). SAP97-silenced or scrambled HEK293 cells were then transiently transfected with $Na_v1.5$ WT or ΔSIV. The current generated by $Na_v1.5$ ΔSIV channels was reduced by 57±9% compared to WT channels in control cells expressing the scrambled shRNA (Figure 6D). In silenced cells (shSAP97), WT and ΔSIV I_{Na} were comparable (49±11% and 57±7% of control values, respectively, Figure 6D). Voltage dependence of activation and inactivation was not significantly different between the four conditions (see Online Figure V). Because β1 subunits are known to associate with Nav1.5,[16] we performed similar experiments using HEK293 cells transfected with $Na_v1.5$ WT or ΔSIV and β1. The results were similar whether the β1 subunit was present or not (Online Figure VIA), without affecting the voltage dependence of activation and inactivation (Online Figure VIB). We finally investigated whether the reduced I_{Na} could be rescued by another protein bearing a PDZ binding domain. As shown in Online Figure VII, overexpression of α1-syntrophin (previously shown to interact with $Na_v1.5$[4]) in silenced cells did not increase I_{Na}.

Silencing of SAP97 in Cultured Rat Atrial Myocytes Reorganizes $Na_v1.5$ Expression

We also investigated whether silencing of SAP97 (Ad shSAP97) alters the organization of $Na_v1.5$ in cardiomyocytes, using a model of cultured atrial myocytes at confluence

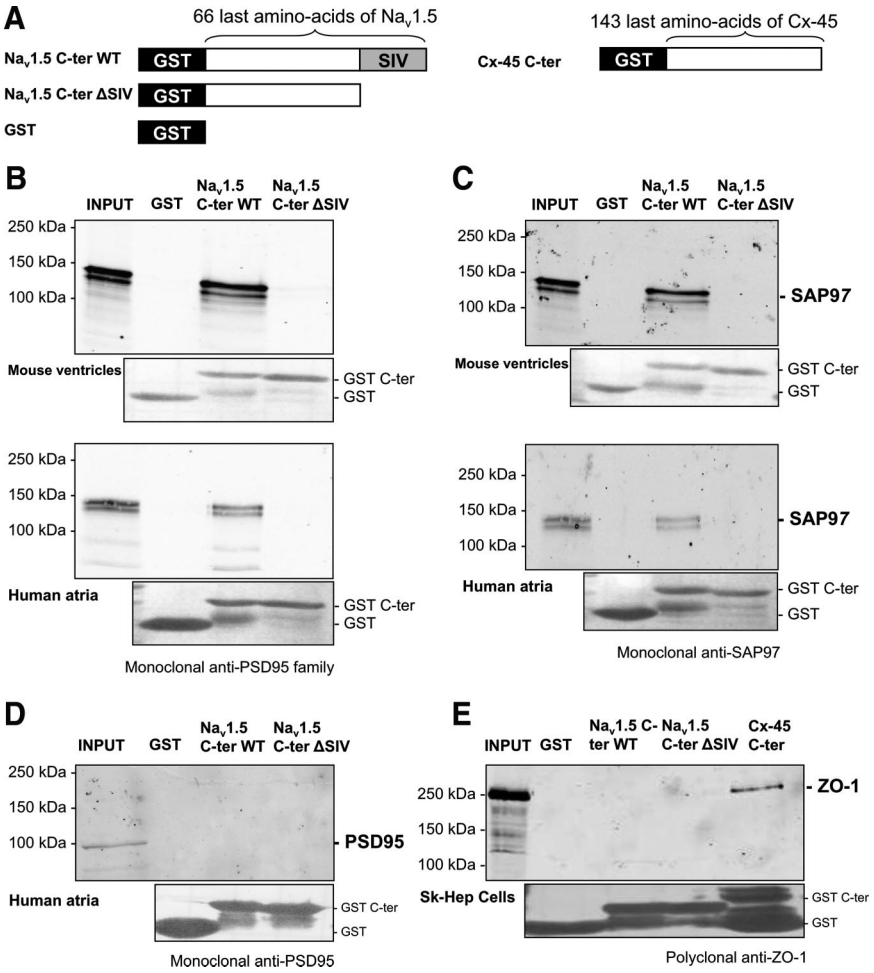

Figure 4. SAP97, but not PSD95, binds to WT $Na_v1.5$ fusion protein in both mouse and human cardiac tissues. A, Schematic representation of the fusion proteins used to perform pull-down assays shown in **B through E**. **B,** Western blots of pulled-down fractions performed on mouse ventricular and human atrial lysates using a monoclonal anti-PSD95-family antibody; 100 μg of lysates were loaded in the input lane. **C,** Same experiment as in panel B, using a monoclonal anti-SAP97 antibody. **D,** Same experiment as in **B** on human atria, using a monoclonal anti-PSD95 antibody. **E,** Western blots of pulled-down fractions performed on Sk-Hep cells using the polyclonal anti–ZO-1 antibody. The **bottom images** are Ponceau stainings indicating that equal amounts of fusion proteins were used. See the Online Data Supplement for full-size blots of Figure 3B and 3C.

stage when cells reestablish highly organized cell-cell contacts as previously shown.[17] Immunostainings on short-term cultured rat atrial myocytes indicate that the total expression of $Na_v1.5$ channels in myocytes transduced with shSAP97 is reduced when compared to cells overexpressing SAP97 (Ad SAP97), and that the localization of the channels at the plasma membrane is reorganized (Online Figure IVA). Costainings of $Na_v1.5$ and syntrophin on rat cardiomyocytes confirm that these 2 proteins are both localized at the cell surface but not at cell-cell contacts where syntrophin is absent

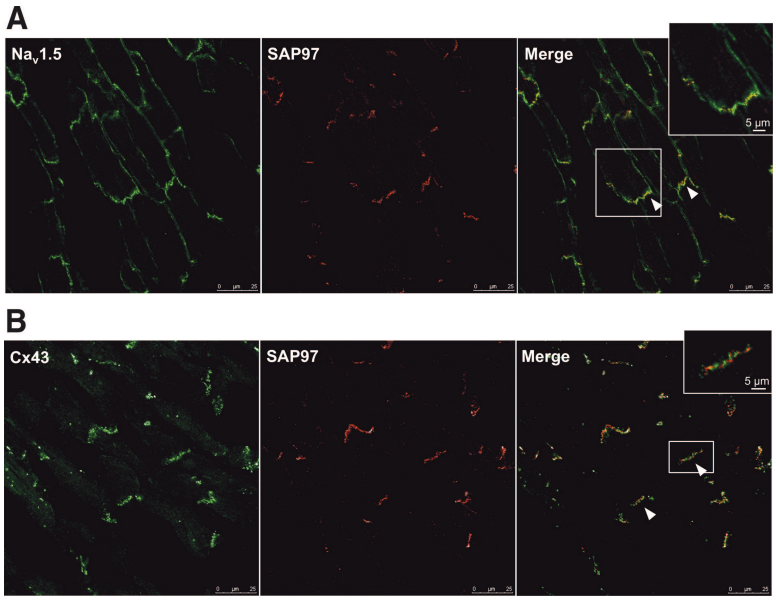

Figure 5. Localization of $Na_v1.5$, SAP97, and Cx43 in rat heart sections. A, Left, $Na_v1.5$ **(green)** both at the lateral membranes and the intercalated discs; middle: SAP97 **(red)** only at the intercalated discs. **Right,** Merge of the 2 images showing close localization of $Na_v1.5$ and SAP97 at the intercalated discs (**white arrowheads**, and magnification in the **inset**). **B, Left,** Cx43 **(green)** only at the intercalated discs. **Middle,** SAP97 **(red)** only at the intercalated discs. **Right,** Merge of the 2 images showing punctuate staining of Cx43 and SAP97 at the intercalated discs (**white arrowheads** and magnification in the **inset**).

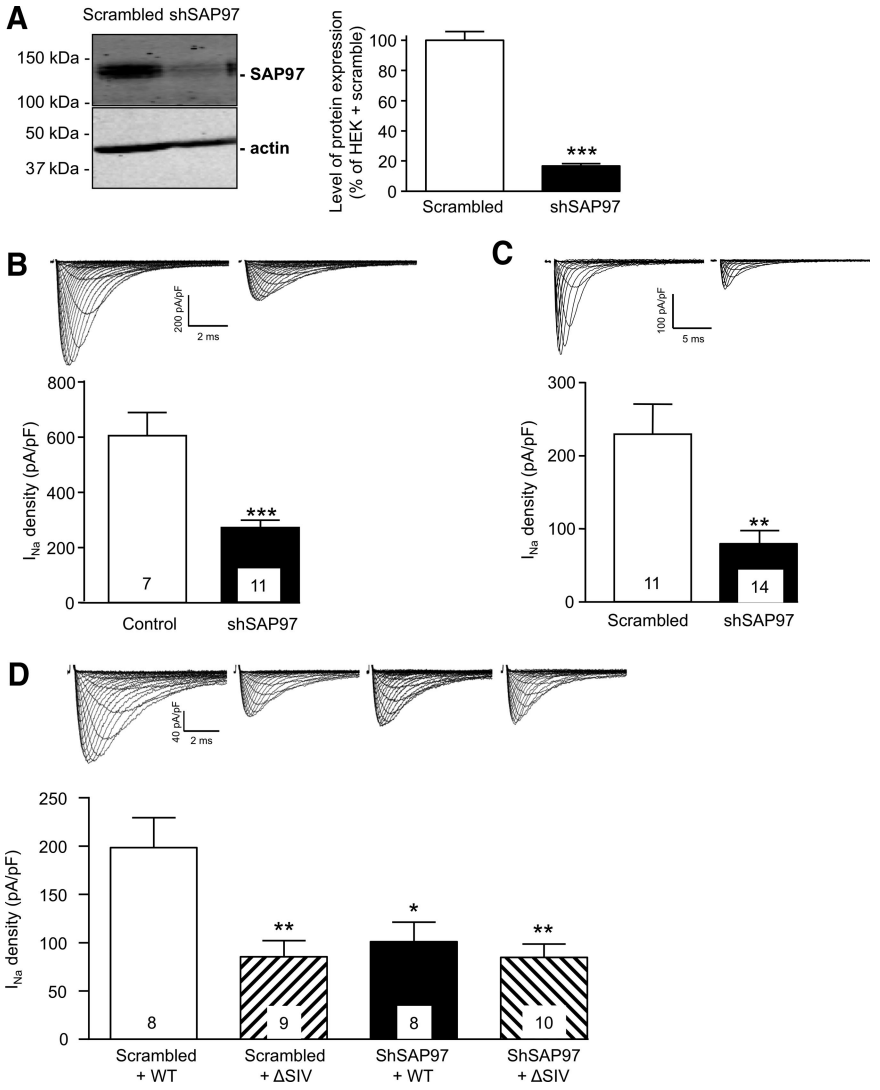

Figure 6. Effect of SAP97 silencing in HEK293 cells and rat adult myocytes. **A,** Western blot of scrambled or SAP97-silenced (shSAP97) HEK293 cell lysates and quantification of the level of protein expression. ***$P<0.001$. **B,** I_{Na} density of HEK293 cells stably expressing $Na_v1.5$ (control: 605.6±83.9 pA/pF) and after SAP97 silencing (shSAP97: 271.8±27.1 pA/pF). ***$P<0.001$ (**inset**: representative currents). **C,** I_{Na} density of scrambled or silenced (ShSAP97) rat adult myocytes (scrambled: 229.3±41.0, shSAP97: 78.9±18.9 pA/pF). **$P<0.01$. **D,** I_{Na} density of scrambled or silenced (ShSAP97) HEK293 cells, transiently transfected with WT or ΔSIV $Na_v1.5$ channels (**inset**: representative currents); *$P<0.05$, **$P<0.01$ (1-way ANOVA and Bonferroni post test compared to the "scrambled+WT" condition). The number of cells is written in the corresponding columns.

(Online Figure IV, B, top). In SAP97 silenced myocytes, syntrophin expression remains unchanged at the level of non–cell-to-cell contacts (Online Figure IVB, bottom).

Expression of $Na_v1.5$ Channels Lacking the SIV-Domain Is Reduced at the Cell Surface of HEK293 Cells and SAP97-Silenced Cells

Electrophysiological data indicate that I_{Na} is dependent on the presence of SAP97 as well as on the SIV motif of $Na_v1.5$. We examined whether the reduced current amplitude was attributable to decreased expression of the channel at the cell surface. Surface biotinylation assays performed on HEK293 cells that had been transiently transfected with $Na_v1.5$ WT or ΔSIV (Figure 7A and 7B) revealed that cell membrane expression of truncated channels was reduced by 27±3% compared to WT channels, without affecting total $Na_v1.5$ protein expression. Similar experiments using scramble-infected HEK293 cells yielded comparable results (35±6% reduction; Figure 7C and 7D). When SAP97-silenced HEK293 cells were transfected with WT or ΔSIV channels, the number of channels expressed at the cell membrane was further reduced (56±5% and 56±6%; Figure 7C and 7D). These results suggest that the decreased I_{Na} measured in SAP97-silenced cells or those with truncated channels may be attributable to reduced cell surface expression of $Na_v1.5$, supporting the idea that SAP97 regulates cell membrane density of $Na_v1.5$. Data presented in Online Figure VIII show that this regulation is independent of the ubiquitin-protein ligase Nedd4-2, which we have previously shown to regulate the number of $Na_v1.5$ channels at the cell surface by interacting with a PY-motif found at the C terminus of the channel.[3]

Discussion

The major findings of the present study are: (1) $Na_v1.5$ is part of at least 2 distinct multiprotein complexes in cardiomyocytes, one localized at the lateral membrane with dystrophin and syntrophin proteins, and the other involving the MAGUK protein SAP97 at the intercalated discs; (2) specific regulation of lateral membrane localization and density of $Na_v1.5$ is dependent on dystrophin expression, the absence of which may underlie conduction slowing observed in dystrophin-deficient hearts; and (3) the absence of the SIV motif of $Na_v1.5$ or depletion of SAP97 results in reduced channel

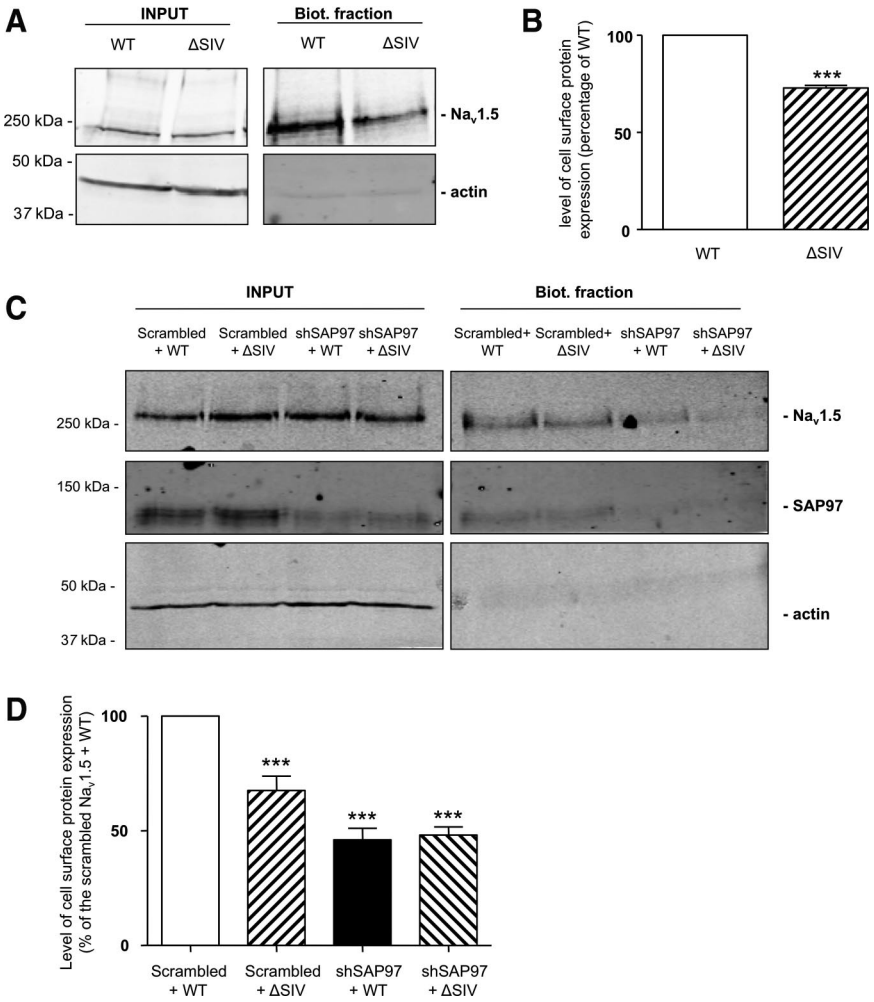

Figure 7. Effect of the absence of the SIV motif and of SAP97 silencing on $Na_v1.5$ channel expression at the plasma membrane. A, Western blot of total protein lysates (**left**, INPUT) and of biotinylated plasma membrane fraction **(right)** of HEK293 cells transfected with $Na_v1.5$ WT or ΔSIV channels showing a decrease of plasma membrane expression of truncated channels. **B,** Quantification of $Na_v1.5$ channel expression at the plasma membrane. ***$P<0.001$; mean of 3 distinct experiments. **C,** Western blot of total protein lysates (**left**, INPUT) and of biotinylated plasma membrane fraction **(right)** of HEK293 cells transfected with $Na_v1.5$ WT or ΔSIV channels in scrambled or SAP97-silenced (shSAP97) HEK293 cells. A decrease in the expression, at the plasma membrane, of truncated channels and in SAP97-silenced cells is observed. The **middle lane** (SAP97) shows the reduction of SAP97 expression in silenced cells. **Bottom,** Absence of actin signal in biotinylated fractions. **D,** Quantification of $Na_v1.5$ channel plasma membrane expression compared to total lysates. ***$P<0.001$; means of 5 distinct experiments.

expression at the cell surface, and a subsequent decrease of I_{Na} in HEK293 cells and adult cardiac myocytes.

Distribution of $Na_v1.5$ Channels in Cardiomyocytes

Studies investigating the localization of $Na_v1.5$ at the cell membrane of cardiac cells have revealed conflicting results. Although many articles have described $Na_v1.5$ stainings at the intercalated discs and lateral membrane of rat,[18,19] mouse,[20] dog,[21] and human[22] cardiomyocytes, other studies have shown almost exclusive expression of the channel at the intercalated discs.[23–25] These discrepancies may be attributable to the alternative use of either heart sections or isolated myocytes, where a reorganization of proteins at the plasma membrane can occur. In a recent study,[26] macropatch recordings of the 2 subcellular domains were performed, and it was concluded that the $Na_v1.5$-mediated current is almost nonexistent at the lateral membrane. The expression, or lack thereof, of $Na_v1.5$ channels at the lateral membranes likely has functional consequences on impulse propagation, as suggested by modeling studies.[25] In the present work, we demonstrate that $Na_v1.5$ channels are present all along the plasma membrane of both rat and mouse cardiomyocytes. This finding is supported by the reduction of lateral $Na_v1.5$ expression in dystrophin-deficient myocytes, with no significant alteration in the expression at the intercalated discs. This observation is consistent with our previous study,[4] in which we observed a ≈50% decrease of total $Na_v1.5$ protein expression in the absence of dystrophin, with a concomitant I_{Na} reduction. Taken together, these observations strongly support the notion that a significant fraction of functional $Na_v1.5$ channels are located outside of the intercalated discs. These lateral membrane channels are likely to play a role in conduction, because their reduction alters ventricular conduction, which is reflected in a widening of the QRS complex in ECG recordings from mdx^{5cv} mice where the hearts are otherwise free from structural remodeling.[4] Confirming this concept, we show here for the first time, using noninvasive optical measurements of conduction velocity from the left ventricle free wall, and by 2 different analysis methods, that impulse propagation is significantly slowed in the transversal direction in dystrophin-deficient hearts that have reduced expression $Na_v1.5$ at the lateral membrane. These findings are in line with those of Baba and coworkers,[21] who showed that dog cardiomyocytes isolated from peri-infarcted zones displayed reduced I_{Na} density, associated with specific loss of the $Na_v1.5$ staining at the lateral membranes only. As the $Na_v1.5$ staining remained unchanged at intercalated discs, the reduction of I_{Na} was proposed to be the cause of altered impulse propagation in the diseased tissue.[21] These observa-

tions are also in agreement with those of a recent study[27] reporting reduced excitability, slowed conduction velocity, and altered $Na_v1.5$ expression in hearts of mdx mice. However, these investigators partly attributed these results to a reorganization of Cx43. Similarly to Sanford and coworkers, we could not confirm this finding in the present study, and found no remodeling of Cx43.[28]

Interaction Between $Na_v1.5$ and SAP97 at Intercalated Discs

The carboxyl terminus of $Na_v1.5$ has several protein–protein interaction domains that associate with numerous partners to regulate channel activity.[2] As aforementioned, we have reported that the last 3 residues of $Na_v1.5$ (SIV) interacts with the DMC, as well as with the protein tyrosine phosphatase PTPH1.[29] Other groups have reported that ion channels bearing a PDZ-domain binding motif interact with members of the MAGUK family in various tissues.[8] Several potassium channels of the K_{ir} and K_v families display PDZ-domain binding motifs that interact with the MAGUK proteins PSD95 or SAP97.[8,12] Our pull-down experiments strongly support the existence of an interaction between $Na_v1.5$ and SAP97 in cardiac tissue via the $Na_v1.5$ SIV motif. These results are supported by a recent study,[30] that suggests that $Na_v1.5$ binds the first PDZ domain of SAP97. In our study, we also describe a close localization of SAP97 and $Na_v1.5$ at intercalated discs. Immunostainings confirm data from Godreau et al[9] who found an enrichment of SAP97 at this subcellular site. These results suggest that SAP97 is involved in targeting or anchoring of $Na_v1.5$ channels to the intercalated discs of cardiomyocytes. Furthermore, SAP97 expression is unaltered in hearts of mdx mice (see Online Figure IX), indicating that the pool of $Na_v1.5$ channels regulated at their PDZ domain-binding motif in the intercalated discs could be independent of the one complexed to syntrophin and DMC at lateral membranes of cardiomyocytes.

Physiological Relevance of the Two Regulating Mechanisms

In addition to the DMC, ankyrin-G has also been shown to interact with and regulate the trafficking of $Na_v1.5$ at the cell membrane of cardiomyocytes.[31,32] Ankyrin-G is primarily expressed at the intercalated discs, with another population at T-tubules; it is therefore unlikely that it is responsible for the specific targeting of $Na_v1.5$ to the 2 compartments observed in our study. Whether the roles of syntrophin-dystrophin and ankyrin-G in trafficking, targeting, and anchoring of $Na_v1.5$ to the lateral membrane are complementary or partly redundant remains to be elucidated. It may be speculated that ankyrin-G is involved in forward trafficking and correct targeting of the channel, and that PDZ-domain proteins anchor it in specific membrane compartments. The exact molecular mechanisms underlying the loss of $Na_v1.5$ expression at the lateral membrane in the absence of dystrophin remains still unclear. Cheng and coworkers[33] recently described several mutations in the gene encoding α1-syntrophin in patients with sudden infant death syndrome. Despite these results, clearly demonstrating the importance of α1-syntrophin in cardiomyocytes function, our data suggest that

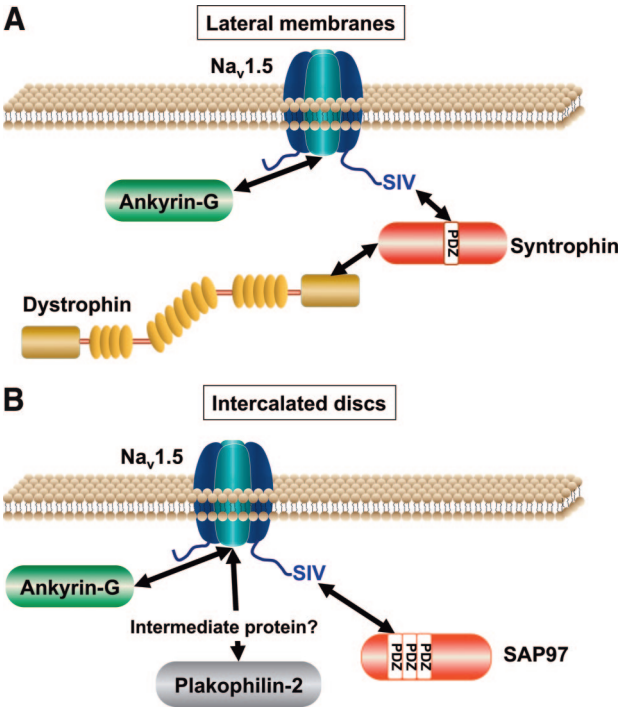

Figure 8. Schematic presentation of $Na_v1.5$ channels of the lateral membrane (A) and the intercalated discs (B). Note that the concept of 2 pools of $Na_v1.5$ channels is most likely an oversimplification. Because ankyrin-G is predominantly found in the T-tubules where little syntrophin-dystrophin is present, a third T-tubular compartment may be proposed.

this protein complex is restricted to the lateral membrane. Sato and coworkers[34] recently demonstrated that I_{Na} is regulated by the protein plakophilin-2, which is enriched at the intercalated discs.[35] Because plakophilin-2 does not contain a PDZ domain, this suggests that $Na_v1.5$ could be differentially regulated by multiple proteins at the intercalated discs including SAP97 and plakophilin-2, similarly to the lateral membrane where it interacts with the DMC and ankyrin-G, within complexes that may or may not be distinct (Figure 8). Deciphering the specific and distinct roles of the different proteins in trafficking and/or anchoring of cardiac ion channels including $Na_v1.5$ to different cellular compartments will be the goal of future experiments.

Limitations of the Study

This study demonstrates the presence of at least 2 different populations of $Na_v1.5$ channels in cardiac cells. However the use of the mdx mouse as a disease model does not allow final conclusions about the physiological function of the 2 different $Na_v1.5$ compartments. The optical mapping data indicate conduction slowing in all directions, and because the exact fiber orientation of the given cardiac substrate is not known, we assume that fiber orientation is similar in WT and mdx hearts at young ages in agreement with previous studies. In addition, our data do not show significant reduction of $Na_v1.5$ expression at the intercalated disc in mdx hearts based on confocal immunofluorescence data. Nevertheless, potential changes of the mdx membrane ultrastructure at this complex site could underlie alterations in intercalated disc excitability

that could not be established specifically here because of resolution limitations of confocal light microscopy. Furthermore, subtle, as yet unrecognized intercellular histological changes in mdx hearts could also contribute to the conduction slowing observed in optical mapping experiments and are subject to the same microscopy diffraction limitations. On the other hand, the present data suggests that SAP97 is predominantly localized in intercalated discs, and that SAP97 protein expression is not different in mdx mouse hearts. However, because immunostaining of SAP97 in mouse heart failed to produce specific staining despite repeated attempts with different antibodies and tissue fixations, possible reorganization of SAP97 cannot be excluded. Finally, potential upregulation or remodeling of connexins other than Cx43 was not addressed in this study.

Conclusions

The present study provides evidence that a fraction of $Na_v1.5$ channels is regulated by the DMC at the lateral myocyte membrane, and a different pool interacts with SAP97 at the intercalated discs of cardiomyocytes. Although the functional relevance of these distinct localizations of the main cardiac sodium channel has yet to be clarified, this study establishes that lateral sodium channels have a role in cardiac impulse propagation. Generation of a cardiac-specific SAP97 knock-out mouse models will likely elucidate the specific roles of this protein in cardiac function. Finally, similar to previous examples of proteins interacting with $Na_v1.5$,[2] genetic variants of SAP97 may be linked to pathological cardiac phenotypes.

Acknowledgments

We are grateful to Maria C. Essers for expert technical assistance.

Sources of Funding

The research leading to these results has received funding from the European Community's Seventh Framework Programme FP7/2007-2013 under grant agreement No. HEALTH-F2-2009-241526, EU-TrigTreat (to H.A., S.L., and S.E.L.). Other support was obtained from grants of the Swiss National Science Foundation to HA (310030_120707), Swiss Heart Foundation, Association Francaise contre les Myopathies (grant 14305), ANR-08-GENO-006-01 (project R08147DS), and by the International Max Planck Research School (IMPRS) for Physics of Biological and Complex Systems (PhD student support to N.R.).

Disclosures

None.

References

1. Zimmer T, Surber R. SCN5A channelopathies - an update on mutations and mechanisms. *Prog Biophys Mol Biol.* 2008;98:120–136.
2. Abriel H. Cardiac sodium channel Nav1.5 and interacting proteins: physiology and pathophysiology. *J Mol Cell Cardiol*. 2010;48:2–11.
3. Rougier J-S, van Bemmelen MX, Bruce MC, Jespersen T, Gavillet B, Apotheloz F, Cordonier S, Staub O, Rotin D, Abriel H. Molecular determinants of voltage-gated sodium channel regulation by the Nedd4/Nedd4-like proteins. *Am J Physiol Cell Physiol.* 2005;288:C692–C701.
4. Gavillet B, Rougier JS, Domenighetti AA, Behar R, Boixel C, Ruchat P, Lehr HA, Pedrazzini T, Abriel H. Cardiac sodium channel Nav1.5 is regulated by a multiprotein complex composed of syntrophins and dystrophin. *Circ Res.* 2006;99:407–414.
5. Blake DJ, Weir A, Newey SE, Davies KE. Function and genetics of dystrophin and dystrophin-related proteins in muscle. *Physiol Rev.* 2002;82:291–329.
6. Kaprielian RR, Stevenson S, Rothery SM, Cullen MJ, Severs NJ. Distinct patterns of dystrophin organization in myocyte sarcolemma and transverse tubules of normal and diseased human myocardium. *Circulation.* 2000;101:2586–2594.
7. Stevenson SA, Cullen MJ, Rothery S, Coppen SR, Severs NJ. High-resolution en-face visualization of the cardiomyocyte plasma membrane reveals distinctive distributions of spectrin and dystrophin. *Eur J Cell Biol.* 2005;84:961–971.
8. Funke L, Dakoji S, Bredt DS. Membrane-associated guanylate kinases regulate adhesion and plasticity at cell junctions. *Annu Rev Biochem.* 2005;74:219–245.
9. Godreau D, Vranckx R, Maguy A, Rucker-Martin C, Goyenvalle C, Abdelshafy S, Tessier S, Couetil JP, Hatem SN. Expression, regulation and role of the MAGUK protein SAP-97 in human atrial myocardium. *Cardiovasc Res*. 2002;56:433–442.
10. Godreau D, Vranckx R, Maguy A, Goyenvalle C, Hatem SN. Different isoforms of synapse-associated protein, SAP97, are expressed in the heart and have distinct effects on the voltage-gated K+ channel Kv1.5. *J Biol Chem.* 2003;278:47046–47052.
11. Leonoudakis D, Conti LR, Anderson S, Radeke CM, McGuire LMM, Adams ME, Froehner SC, Yates JR III, Vandenberg CA. Protein trafficking and anchoring complexes revealed by proteomic analysis of inward rectifier potassium channel (Kir2.x) associated proteins. *J Biol Chem.* 2004;279:22331–22346.
12. El-Haou S, Balse E, Neyroud N, Dilanian G, Gavillet B, Abriel H, Coulombe A, Jeromin A, Hatem SN. Kv4 potassium channels form a tripartite complex with the anchoring protein SAP97 and CaMKII in cardiac myocytes. *Circ Res*. 2009;104:758–769.
13. Lai HC, Jan LY. The distribution and targeting of neuronal voltage-gated ion channels. *Nat Rev Neurosci.* 2006;7:548–562.
14. Appert-Collin A, Cotecchia S, Nenniger-Tosato M, Pedrazzini T, Diviani D. The A-kinase anchoring protein (AKAP)-Lbc-signaling complex mediates alpha1 adrenergic receptor-induced cardiomyocyte hypertrophy. *Proc Natl Acad Sci U S A.* 2007;104:10140–10145.
15. Kausalya PJ, Reichert M, Hunziker W. Connexin45 directly binds to ZO-1 and localizes to the tight junction region in epithelial MDCK cells. *FEBS Lett.* 2001;505:92–96.
16. Malhotra JD, Chen C, Rivolta I, Abriel H, Malhotra R, Mattei LN, Brosius FC, Kass RS, Isom LL. Characterization of sodium channel alpha- and beta-subunits in rat and mouse cardiac myocytes. *Circulation.* 2001;103:1303–1310.
17. Abi-Char J, El-Haou S, Balse E, Neyroud N, Vranckx R, Coulombe A, Hatem SN. The anchoring protein SAP97 retains Kv1.5 channels in the plasma membrane of cardiac myocytes. *Am J Physiol Heart Circ Physiol*. 2008;294:H1851–H1861.
18. Scriven DR, Dan P, Moore ED. Distribution of proteins implicated in excitation-contraction coupling in rat ventricular myocytes. *Biophys J*. 2000;79:2682–2691.
19. Yarbrough TL, Lu T, Lee HC, Shibata EF. Localization of cardiac sodium channels in caveolin-rich membrane domains: regulation of sodium current amplitude. *Circ Res*. 2002;90:443–449.
20. Haufe V, Camacho JA, Dumaine R, Gunther B, Bollensdorff C, Segond von Banchet G, Benndorf K, Zimmer T. Expression pattern of neuronal and skeletal muscle voltage-gated Na+ channels in the developing mouse heart. *J Physiol.* 2005;564(Pt 3):683–696.
21. Baba S, Dun W, Cabo C, Boyden PA. Remodeling in cells from different regions of the reentrant circuit during ventricular tachycardia. *Circulation.* 2005;112:2386–2396.
22. Chandler NJ, Greener ID, Tellez JO, Inada S, Musa H, Molenaar P, DiFrancesco D, Baruscotti M, Longhi R, Anderson RH, Billeter R, Sharma V, Sigg DC, Boyett MR, Dobrzynski H. Molecular architecture of the human sinus node: insights into the function of the cardiac pacemaker. *Circulation.* 2009;119:1562–1575.
23. Maier SK, Westenbroek RE, Schenkman KA, Feigl EO, Scheuer T, Catterall WA. An unexpected role for brain-type sodium channels in coupling of cell surface depolarization to contraction in the heart. *Proc Natl Acad Sci U S A.* 2002;99:4073–4078.
24. Maier SKG, Westenbroek RE, McCormick KA, Curtis R, Scheuer T, Catterall WA. Distinct subcellular localization of different sodium channel {alpha} and {beta} subunits in single ventricular myocytes from mouse heart. *Circulation.* 2004;109:1421–1427.

25. Kucera JP, Rohr S, Rudy Y. Localization of sodium channels in intercalated disks modulates cardiac conduction. *Circ Res.* 2002;91:1176–1182.
26. Verkerk AO, van Ginneken ACG, van Veen TAB, Tan HL. Effects of heart failure on brain-type Na+ channels in rabbit ventricular myocytes. *Europace.* 2007;9:571–577.
27. Colussi C, Berni R, Rosati J, Straino S, Vitale S, Spallotta F, Baruffi S, Bocchi L, Delucchi F, Rossi S, Savi M, Rotili D, Quaini F, Macchi E, Stilli D, Musso E, Mai A, Gaetano C, Capogrossi MC. The histone deacetylase inhibitor suberoylanilide hydroxamic acid reduces cardiac arrhythmias in dystrophic mice. *Cardiovasc Res.* 2010;87:73–82.
28. Sanford JL, Edwards JD, Mays TA, Gong B, Merriam AP, Rafael-Fortney JA. Claudin-5 localizes to the lateral membranes of cardiomyocytes and is altered in utrophin/dystrophin-deficient cardiomyopathic mice. *J Mol Cell Cardiol.* 2005;38:323–332.
29. Jespersen T, Gavillet B, van Bemmelen MX, Cordonier S, Thomas MA, Staub O, Abriel H. Cardiac sodium channel Nav1.5 interacts with and is regulated by the protein tyrosine phosphatase PTPH1. *Biochem Biophys Res Commun.* 2006;353:1456–1463.
30. Stiffler MA, Chen JR, Grantcharova VP, Lei Y, Fuchs D, Allen JE, Zaslavskaia LA, MacBeath G. PDZ domain binding selectivity is optimized across the mouse proteome. *Science.* 2007;317:364–369.
31. Lowe JS, Palygin O, Bhasin N, Hund TJ, Boyden PA, Shibata E, Anderson ME, Mohler PJ. Voltage-gated Nav channel targeting in the heart requires an ankyrin-G dependent cellular pathway. *J Cell Biol.* 2008;180:173–186.
32. Mohler PJ, Splawski I, Napolitano C, Bottelli G, Sharpe L, Timothy K, Priori SG, Keating MT, Bennett V. A cardiac arrhythmia syndrome caused by loss of ankyrin-B function. *Proc Natl Acad Sci U S A.* 2004;101:9137–9142.
33. Cheng J, Van Norstrand DW, Medeiros-Domingo A, Valdivia C, Tan BH, Ye B, Kroboth S, Vatta M, Tester DJ, January CT, Makielski JC, Ackerman MJ. {alpha}1-Syntrophin mutations identified in sudden infant death syndrome cause an increase in late cardiac sodium current. *Circ Arrhythmia Electrophysiol.* 2009;2:667–676.
34. Sato PY, Musa H, Coombs W, Guerrero-Serna G, Patino GA, Taffet SM, Isom LL, Delmar M. Loss of plakophilin-2 expression leads to decreased sodium current and slower conduction velocity in cultured cardiac myocytes. *Circ Res.* 2009;105:523–526.
35. Oxford EM, Everitt M, Coombs W, Fox PR, Kraus M, Gelzer AR, Saffitz J, Taffet SM, Moise NS, Delmar M. Molecular composition of the intercalated disc in a spontaneous canine animal model of arrhythmogenic right ventricular dysplasia/cardiomyopathy. *Heart Rhythm.* 2007;4:1196–1205.

Novelty and Significance

What Is Known?

- Cardiac sodium channel $Na_v1.5$ plays an essential role in action potential initiation and impulse propagation.
- Hundreds of mutations in the gene encoding $Na_v1.5$, *SCN5A*, have been found in patients with various cardiac disorders such as congenital long QT syndrome, Brugada syndrome, and dilated cardiomyopathy.
- Many regulatory proteins have been found to interact with $Na_v1.5$ and form macromolecular complexes.

What New Information Does This Article Contribute?

- Cardiac sodium channels are parts of at least 2 distinct macromolecular complexes in cardiac cells: one localized at lateral membranes with the dystrophin complex and one at the intercalated discs.
- Absence of dystrophin leads to a specific downregulation of lateral $Na_v1.5$ channels and impulse propagation slowing.
- The scaffolding protein SAP97, which is predominantly found at the intercalated discs, interacts with $Na_v1.5$ and regulates its membrane density, hence forming another macromolecular complex.

Previously, we have demonstrated that $Na_v1.5$ forms a macromolecular complex with dystrophin and syntrophin proteins. However because dystrophin is absent from the intercalated discs, we investigated the composition of the complex in this compartment. We found that $Na_v1.5$ channels are a parts of distinct macromolecular complexes in cardiomyocytes, one localized at the lateral membrane with the dystrophin/syntrophin complex, and the other involving the scaffolding protein SAP97 at the intercalated discs and that specific regulation of lateral membrane localization and density of $Na_v1.5$ is dependent on dystrophin, the absence of which underlie conduction slowing observed in dystrophin-deficient hearts. We report that depletion of SAP97 reduces channel expression at the cell surface and decreases sodium current. These findings suggest that there is not "one" sodium channel in cardiac cells, but multiple $Na_v1.5$ channels that are differentially regulated in the different membrane compartments. These differences may underlie the variability of the cardiac phenotypes observed with genetic dysfunction of the cardiac sodium channel and could impart specific roles to different macromolecular complexes in normal and diseased heart.

CIRCRESAHA/2009/210153
Revised Version
Submitted on December 2, 2010

Regular Article

Supplement Material

SAP97 and dystrophin macromolecular complexes determine two pools of cardiac sodium channels $Na_v1.5$ in cardiomyocytes

Séverine Petitprez[1,2*], PhD, Anne-Flore Zmoos[1*], MSc , Jakob Ogrodnik[1], PhD, Elise Balse[2], PhD, Nour Raad[3,4], MD, Said El-Haou[2], PhD, Maxime Albesa[1], MSc, Philip Bittihn[3], MSc, Stefan Luther[3,5], PhD, Stephan E. Lehnart[4,6], MD, PhD, Stéphane N. Hatem[2], MD, PhD, Alain Coulombe[2], PhD, and Hugues Abriel[1], MD, PhD

Petitprez - Two pools of $Na_v1.5$ channels

[1] Department of Clinical Research, University of Bern, Switzerland
[2] INSERM U956, Université Pierre et Marie Curie-Paris 6, France
[3] Max Planck Institute for Dynamics and Self-Organization, Göttingen, Germany
[4] Dept. of Cardiology & Pulmonology, University Medical Center Göttingen, Germany
[5] Dept. of Biomedical Sciences, Cornell University, Ithaca, NY, USA
[6] Center for Biomedical Engineering and Technology, University of Maryland Baltimore, Baltimore MD 21201, USA

[152] Ion channels/membrane transport
[130] Animal models of human disease

*These authors contributed equally to this study

Correspondence to:
Dr. Hugues Abriel, MD PhD
University of Bern, Department of Clinical Research
Murtenstrasse, 35, 3010 Bern, Switzerland
Phone: 41-31-6320928
Fax: 41-31-6320946
Email: Hugues.Abriel@dkf.unibe.ch

Methods

Cardiac tissue samples and myocyte isolation

The experimental procedures were approved by the ethical commission on clinical research of the faculty of medicine of the University of Lausanne. Human right atrial samples were collected from patients in normal sinus rhythm undergoing coronary bypass surgery. The tissue was placed in ice cold PBS for transportation before being processed in our laboratory. C57BL/6 mice purchased at Janvier (Le Genest St Isle, France), and mdx^{5cv} mice were anesthetized by intraperitoneal injection of 100 µl of pentobarbital (50 mg/ml) and 100 µl of heparin (Liquemin 5000 U.I./ml, Roche, Basel, Switzerland). Male Sprague rats (kind gift of Dr. D.Diviani, University of Lausanne) were anesthetized with 1.5L O_2 / 5% isoflurane. A thoracotomy was performed and the cardiac ventricles were excised, rinsed with ice cold PBS and either frozen in liquid nitrogen or directly used for an experiment.

For patch-clamp experiments, Wistar rats (handled in accordance with guidelines for the care and use of laboratory animals published by the US National Institutes of Health) were anesthetized by intraperitoneal injection of heparin (0.1 ml/100 mg of body weight) and pentobarbital (0.15 ml/100 g of body weight). Atria were dissected out and chopped into small pieces in Tyrodebicarbonate solution containing (mM): 120 NaCl, 5.6 KCL, 0.6 NaH_2PO_4, 1.1 $MgCl_2$, 11.1 glucose and 24 $NaHCO_3$, pH adjusted to 7.6 by bubbling with carbogen gas (95% O2, 5% CO_2), and supplemented with 30 mM BDM, 10 mM taurine and 0.5 mM EGTA. Tissue fragments were then transferred into a Cell-Stir and predigested for 15 minutes with a mixture of type XXIV protease (20 U/ml, Sigma) and type V collagenase (10 U/ml, Sigma) diluted in calcium-free Krebs solution containing (mM): 10 HEPES, 35 NaCl, 10 glucose, 134 sucrose, 16 Na_2HPO_4, 25 $NaHCO_3$, 4.75 KCl, 1.2 H_2PO_4 and 1% BSA. The supernatant was discarded and tissue pieces were then subjected to four or five successive baths of 10 minutes each with type V collagenase (685 U/ml). Each supernatant was centrifuged to remove the enzyme and the pellets were resuspended in calcium-free Tyrode buffer containing (mM): 135 NaCl, 20 glucose, 10 HEPES, 4 KCl, 1 Na_2HPO_4, 2 $MgCl_2$ and supplemented with 10 mM BDM and 1% BSA. At the end of the digestion, resuspended pellets were pooled, centrifuged and resuspended in 3 ml of Tyrode solution containing 0.2 mM calcium for 5 minutes. To gradually increase the calcium concentration, the same volume of culture medium was added and the cells were incubated for another 5 minutes. After a final centrifugation step, the pellets were resuspended in M199 medium (Gibco) with 100 IU/ml penicillin and 100 µg/ml streptomycin, supplemented with 1% FBS (Gibco) and 1/1000 ITS (Sigma). Isolated cells were cultured under standard conditions (37°C, 5% CO_2) until patch-clamp recordings were performed.

Isolation of mouse ventricular myocytes. Single cardiomyocytes were isolated according to established enzymatic procedures as previously described[1] from 3 month old WT (C57BL/6) and *mdx* (C57BL/10ScSn-*Dmd*^{mdx}) mice (Jackson Laboratories, Bar Harbor, ME, USA). Briefly, mice were euthanized by cervical dislocation. Following intraventricular administration of heparin (500 U through the apex; Biochrom, Berlin, Germany), hearts were rapidly excised, cannulated and mounted on a Langendorff column for retrograde perfusion at 37°C. Hearts were rinsed free of blood with nominally Ca^{2+}-free solution containing (in mmol/L): 135 NaCl, 4 KCl, 1.2 $MgCl_2$, 1.2 NaH_2PO_4, 10 HEPES, 11 glucose, pH 7.4 (NaOH adjusted), and subsequently digested by a solution supplemented with 50 µM Ca^{2+} and collagenase type II (0.6 mg/mL, Worthington, Switzerland) for 15 minutes. Following digestion, the atria were removed and the ventricles transferred to phosphate buffered saline, PBS (pH 7.4, Gibco, Basel, Switzerland), where they were minced into small pieces. Cardiomyocytes were liberated by gentle trituration of the digested ventricular tissue, filtered through a 200 µm nylon mesh and washed twice in PBS.

Cell preparation, transfection and infection

Human Embryonic Kidney (HEK293) and Sk-Hep cells were cultured in DMEM (Gibco) supplemented with 10% FBS, 0.2% glutamine and gentamicin (20 mg/mL) or geneticin (400 µg/mL), at 37°C in a 5% CO_2 incubator.

Silencing and lentiviruses

For preliminary silencing studies, HEK293 cells stably expressing $Na_v1.5$ channels were transfected using lipofectamin™ (Invitrogen) with 0.6 µg EBO-pCD-Leu2-CD8 cDNA encoding CD8 antigen as a reporter gene and 1.8 µg of either SAP97 silencing oligos (cloned in pSUPER) or a scramble sequence of these oligos or pSUPER (empty vector). The following sequence was used to silence SAP97: SAP97-shRNA: 5'-GATATCCAGGAACATAAAT-3' Scramble-shRNA: 5'-CCATAATACAAGGTATAA-3' (sequences from Gardner and co-workers). Then, VSV-G pseudotyped lentiviruses were produced by co-transfecting HEK293-T cells with 20 µg of the pSD28-GFP or pAB286.1 vectors containing the SAP97 shRNA cassette, 15 µg of pCMVDR8.91, and 5 µg of pMD2.VSVG by using the calcium phosphate method (empty plasmids: kind gift of D.Diviani group). Culture medium was replaced by serum-free DMEM 12h after transfection. Cell supernatants were collected 48h later and filtered through a 0.45-µm filter unit. HEK293 cells and HEK293 cells stably expressing $Na_v1.5$ channels were infected with lentiviruses containing shRNA against SAP97, the scramble sequence or the empty vector. Two days after infection, puromycin was added to the culture medium at a final concentration of 4 µg/ml. After 4 days of selection, puromycin-resistant cells were collected and amplified in selective medium containing puromycin at a final concentration of 4 µg/ml.
To silence rat cardiomyocytes the following shRNA sequences were used: ShSAP97: 5'-CCCAAATCCATGGAAAATA-3' (conserved sequence between SAP97 isoforms), or scramble: 5'-GTATAATACACCGCGCTAC-3'. These oligos were cloned into the psiSTRIKES™ hMGFP vector which renders transfected myocyte a green fluorescent cells (Promega, Fr). Following the dissociation, adult cardiomyocytes were cultured for 1 night in a 1% CO_2 incubator before transfection with either scrambled or SAP97 shRNA using a liposomal approach (Lipofectamine 2000, Invitrogen).

Transfection

For patch clamp experiments, HEK293 cells were transiently transfected using calcium phosphate with 0.3 µg of GFP-tagged $Na_v1.5$ (kind gift from Dr. T. Zimmer, University of Jena, Jena, Germany) or GFP-tagged $Na_v1.5\Delta SIV$. For experiments addressing the roles of Nedd4-2 or Syntrophin, 1.4 µg of Nedd4-2 was added to 0.3 µg of $Na_v1.5$ WT or YA and 1.4 µg of Syntrophin or empty pcDNA3.1 plasmid were added to 0.3 µg of GFP-tagged $Na_v1.5$. 0.6 µg of pIRES-hβ1-CD8 cDNAs encoding hβ1 subunit (CD8 antigen as a reporter gene) or 0.6 µg EBO-pCD-Leu2-CD8 cDNA were used.

Protein extraction

Frozen human atrial appendages or fresh mouse ventricles were transferred into Lysis Buffer (50 mM Tris pH 7.5, 150 mM NaCl, 1 mM EDTA, 1 mM PMSF and Complete® protease inhibitor cocktail from Roche). Tissues were then homogenized using a Polytron. Triton Tx-100 was added to achieve a final concentration of 1% and solubilisation occurred by rotating for 1h30 at 4°C. HEK293 or Sk-Hep cells were washed with Phosphate Buffer Saline (PBS, Invitrogen) and lysed in Lysis Buffer containing 1% Tx-100 lysed for 45 minutes at 4°C on a wheel. The soluble fractions from a subsequent 15-min centrifugation at 13,000 g (4°C) were then used for the experiments. In order to load each lane of the SDS-page with equivalent amounts of total

protein, the protein concentration of each lysate was measured in triplicate by Bradford assay using a BSA standard curve.

Pull-down assays

cDNAs encoding the last 66 amino acids of $Na_v1.5$ WT and S2014Stop were cloned into pGEX-4T1 (Amersham Bioscience, Piscataway, USA). Expression of GST-fusion proteins in *E.Coli* K12 cells was induced with 0.5 mM IPTG for 2 h at 30°C. Cells were harvested by centrifugation and re-suspended in lysis buffer (20 mM Tris pH 7.5, 250 mM NaCl, 0.5% NP40, 1 mM EDTA, 1 mM PMSF, 0.2 mg/ml DNASE I (Roche) and 0.2 mg/ml Lysozyme (Roche)). After bacterial lysis, fusion proteins were purified on Glutathione-Sepharose beads (Amersham Bioscience). The soluble fractions obtained after applying the protein extraction protocol (see above) were incubated with GSH-sepharose beads containing either GST or the GST fusion protein off the beads. After four washes in Lysis Buffer, samples were re-suspended with 2.5x Sample Buffer containing 60 mM 1,4-Dithiothreitol (Uptima) and boiled five minutes at 95°C. Beads were removed from the samples and the resulting pulled-down proteins were analyzed by Western blot as described below.

Biotinylation Assay

HEK293 cells silenced for SAP97 as well as control cells (scrambled) were transfected either with the WT or truncated $Na_v1.5$ channels. 48h after transfection, cells were washed twice with PBS and biotinylated for 30 minutes at 4°C using PBS containing 2.5mg of EZ Link Sulfo-NHS-SS-Biotin. Plates were washed twice with PBS-200mM Glycine (to quench unlinked biotin) and twice with PBS. Cells were then lysed for one hour at 4°C with Biotinylation Lysis Buffer (50 mM Hepes pH7.4; 150 mM NaCl; 1.5 mM $MgCl_2$; 1 mM EGTA; 10% Glycerol; 1% Triton X-100; 1.2mg/ml N-Ethyl-maleimide and Complete® protease inhibitor cocktail from Roche). After centrifugation, supernatants were incubated with 30 µl of Streptavidin-Sepharose beads (GE healthcare, Waukesha, Wisconsin, USA) for 2 hours at 4°C and pelleted by centrifugation. After 5 washes with Biotinylation Lysis Buffer containing 100 mM PMSF the samples were warmed for 30 minutes at 37°C in 2.5x Sample Buffer (containing 60 mM DTT). Biotinylated proteins were then analysed by Western Blot as described below.

Western blot

Proteins were separated on a 5-15% acrylamide SDS-PAGE, then transferred to a nitrocellulose membrane and incubated with primary antibodies followed by infrared IRDye™ secondary antibodies. Proteins were detected using the Odyssey® Infrared Imaging System (Bad Homburg).

Immunohistochemistry on rat and mouse heart sections

Hearts from C57BL/6 male mice at 10 weeks of age or Sprague male rats at 7 weeks of age were longitudinally cut and embedded in Tissue-Tek® O.C.T™ Compound (Sakura Finetek, Zoeterwoude, Netherland). Frozen sections of 5 µm thickness were stored at -80°C until further use. Cryosections were let to dry at room temperature (RT) for about 15 minutes before starting the immunostainings. Except when indicated, all further manipulations were performed at room temperature (~25°C). Tissue sections were rehydrated in PBS before being fixed using either 2% paraformaldehyde or cold aceton for 10 minutes depending on the primary antibody. Cryosections were rinsed in PBS and then blocked for one hour in PBS containing 0.5% Triton X-100, 1% BSA and 10% goat serum. Frozen heart slices were incubated with primary antibodies diluted in PBS containing 0.5% Triton X-100, 1% BSA and 3% goat serum for 2h. Tissues slices were rinsed with PBS and then incubated for 1 hour with secondary antibodies (diluted in the same solution as the primary antibody). After washes in PBS, Fluorsave (Merck)

was added to the cryosections. Frozen heart slices were then covered with a glass coverslip and kept at 4°C till further analysis. For control experiments, primary antibodies were omitted. Immunostainings were analyzed using a confocal microscope (Leica SP5 AOBS).

Immunocytochemistry of isolated mouse ventricular myocytes. Cell suspensions containing WT and *mdx* cardiomyocytes respectively were mixed, and cells were plated on laminin-coated glass cover slips and allowed to adhere for 1h. Cardiomyocytes were fixed for 10 min with 4% paraformaldehyde in PBS, and free aldehyde groups were quenched with 150 mM glycine for 10 min. Cells were washed in PBS (2 × 10 min) and subsequently permeabilized with 0.5% Tween 20 for 30 min. After the permeabilization solution had been washed out with PBS (3 × 10 min), WT and *mdx* cardiomyocytes were labelled with antibodies directed against rabbit $Na_v1.5$ and mouse dystrophin by incubation overnight at 4°C in primary antibody buffer (1% BSA, 5% goat serum in PBS). Following washout of excess primary antibodies (3 × 10 min PBS), cells were incubated with secondary antibodies for 1h and washed with PBS (3 × 10 min) before the cover slips were mounted onto frosted slides in a solution composed of 90% FluorSave Reagent (Calbiochem, La Jolla, CA, USA) and 10% 10X PBS.

Immunocytochemistry and 3D-microscopy of cultured atrial myocytes. Adult atrial myocytes were isolated from rat atria as described previously[2] and transduced the day after with adenoviruses in order to either over-express (Ad SAP97, personal production) or silence SAP97 (Ad shSAP97[3]). Transduction with an Ad shß-Gal was used as control. Three days later, cells were fixed for 10 minutes with acetone. Coverslips were incubated for one hour in blocking buffer (PBS, 1% BSA, 0.5% Triton X100, 10% goat serum and 10% chicken serum) before overnight incubation with primary antibodies (diluted in blocking buffer: PBS, 1% BSA, 0.5% Triton X100 and 3% goat serum and 10% chicken serum). Indirect immunofluorescence was performed using secondary antibodies while nuclei were stained with the DAPI dye. Images were acquired with an Olympus epifluorescent microscope (60X, UPlanSApo, 0.17) equipped with a cooled CoolSnap camera (Roper-Scientific). Sections of 0.2 µm thickness were collected using a piezoelectric system driven by the Metamorph software (Molecular Devices) and supplemented with the 3D-deconvolution module. For each sample, 3 consecutive z-images were thresholded to similar levels and z-projections were carried on using the ImageJ software. Brightfield images were also acquired to provide information on cell shape and cell membranes.

Antibodies

The following antibodies were used: Polyclonal anti-actin (A 2066) monoclonal anti-dystrophin (clone MANDYS8) obtained from SIGMA (Buchs, Switzerland). Polyclonal antibody recognizing human/rat $Na_v1.5$ was purchased from Alomone labs (ASC-005; Jerusalem, Israel). Monoclonal anti-PSD-95 family (recognizing PDZ domains of PSD95, chapsin110 and SAP97) used for biochemical assays were from United States Biological (clone 0.T.124; Swampscott, Massachusetts, USA), and those used for immunohistochemistry were from UC Davis/NIH NeuroMab Facility. Polyclonal anti-PSD95 was from Abcam (ab12093; Cambridge, England). Monoclonal anti-SAP97, used for biochemistry and immunohistochemistry on isolated rat myocytes, was obtained from StressGen (VAM-PS005; Ann Arbor, Michigan, USA) and that used for immunohistochemistry was obtained from UC Davis/NIH NeuroMab Facility (antibodies were developed at NeuroMab, supported by NIH grant U24NS050606 and maintained by the Department of Neurobiology, Physiology and Behavior, College of Biological Sciences, University of California, Davis, CA 95616). Polyclonal anti-ZO-1 was purchased from ZYMED Laboratories (ZMD.436; Carlsbad, California, USA). Monoclonal pan-syntrophin (recognizing

alpha 1, beta 1 and beta 2 subunits of syntrophin) was obtained from Affinity Bioreagents (Thermo Fisher Scientific, Rockford, Illinois, USA). A polyclonal anti-Connexin-43 was from Abcam (ab66151) and a monoclonal form from Chemicon (Mab3068; Millipore; Billerica, Massachusetts, USA).
In Western blot experiments, infrared IRDye™ (680 or 800 CW) secondary antibodies were purchased from LI-COR Biosciences (Bad Homburg, Germany). Secondary antibodies used for immunohistostainings were the following: Fluorescein (FITC)-conjugated anti-rabbit (711-095-152) from Jackson Immunoresearch laboratories (West Grove, Pennsylvania, USA); and Alexa Fluor® 647 anti-mouse (A-31571), goat anti-mouse-Alexa 488 and chicken anti-rabbit-Alexa 594 from Invitrogen (Basel, Switzerland).

Electrophysiology

For patch-clamp recordings, pClamp software, version 8 (Axon Instruments, Union City, CA) and a VE-2 (Alembic Instruments, Montreal, QC, Canada) were used. Data were analyzed using pClamp software, version 8 (Axon Instruments) and KaleidaGraph (Synergy Software, Reading, PA). Patch-clamp recordings of HEK cells were carried-out using an internal solution containing (mmol/L) CsCl 60; Cs aspartate 70; EGTA 11; $MgCl_2$ 1; $CaCl_2$ 1; HEPES 10; and Na_2-ATP 5, pH 7.2 with CsOH and external solution NaCl 50; n-methyl-D-glutamine 80; $CaCl_2$ 2; $MgCl_2$ 1.2; CsCl 5; HEPES 10; and glucose 5, pH 7.4 with CsOH. Measurements were done in the whole-cell configuration. Using these solutions, 5 min after rupturing the membrane, no significant alterations of the availability curve nor the peak current were observed. Holding potentials were -100 mV and no leak subtraction was performed. The resistance of the pipettes was in the range of 1.9–2.9 MΩ. We used only data from cells where the access resistance remained stable over the entire duration of the experiment. Cells for which signs of poor voltage-clamp control such as delayed inflections of the current or discontinuities in the peak I_{Na} vs. Vm curve were not analyzed. Measurements were carried out at room temperature (~25°C).
Peak currents were measured at -20mV during a current-voltage protocol and I_{Na} densities (pA/pF) were obtained by dividing the peak I_{Na} by the cell capacitance obtained from the pClamp function. Activation properties were determined from I/V relationships (see inserted protocols in figures) by normalizing peak I_{Na} to driving force and maximal I_{Na}, and plotting normalized conductance vs Vm. Voltage-dependence of steady-state inactivation was obtained by plotting the normalized peak current (25-ms test pulse to -20 mV after a 500-ms conditioning pulse) vs Vm. For the voltage-dependence of steady-state activation and inactivation (fast and slow) curves, the data from individual cells were fitted with Boltzmann relationship, $y(Vm) = 1/(1+\exp[(Vm-V_{1/2})/K])$, in which y is the normalized current or conductance, Vm is the membrane potential, $V_{1/2}$ is the voltage at which half of the channels are activated or inactivated, and K is the slope factor.

Isolated rat adult atrial cardiomyocytes were patched with an internal solution containing (mM) NaCl 10, CsCl 130, $CaCl_2$ 1, EGTA 10, HEPES 10, MgATP 5 and D-glucose 10, pH 7.2 with CsOH, and an external perfusion solution containing NaCl 80, CsCl 50, $CoCl_2$ 2.5, $CaCl_2$ 2, 4-AP 5, HEPES 10 et glucose 10; pH 7.4 with CsOH. During the recordings, myocytes were incubated in a Tyrode solution containing (mM): NaCl 135, KCl 4, $MgCl_2$ 2, $CaCl_2$ 2, HEPES 10, NaH_2PO_4 1, Na-pyruvate 2.5, and D-glucose 20, pH 7.4 with NaOH. Ionic currents were recorded with a patch-clamp amplifier (Axopatch 200A, Molecular Devices). Patch pipettes (Corning Kovar Sealing code 7052, WPI) had resistances of 1.5 to 2 MΩ. Holding potentials were -140mV and currents were recorded every 5 or 10mV from -90mV to 60mV at 0.2Hz and digitized with a DigiData 1200 (Molecular Devices). Data were acquired and analyzed with Acquis-1 software (G. Sadoc, CNRS, Gif/Yvette, France).

Optical mapping of the mouse left ventricle

Data were obtained from young adult (14-16 weeks) male wild-type (C57BL/10ScSn; n=6) and mdx (C57BL/10ScSn-*Dmd*^{mdx}/J; n=8) mouse hearts. All animal care conformed with institutional guidelines and German laws for the Care and Use of Laboratory Animals. Mice were obtained from The Jackson Laboratory (Bar Harbor, MN).

High-resolution optical mapping studies were performed in Langendorff perfused mouse hearts extracted from euthanized, heparinized wild-type and mdx mice as indicated. The aorta of the intact hearts was carefully cannulated using a 22 G cannula and connected to a custom-made perfusion setup. The heart was perfused at 2-3 ml/min with O_2-saturated Tyrode solution containing (mmol/L): NaCl 130, $NaHCO_3$ 24, KH_2PO_4 1.2, $MgCl_2$ 1, glucose 5.6, KCl 4, $CaCl_2$ 1.8, 37°C, pH 7.4; as well as insulin (5 IU/L), blebbistatin (5 µmol/L), and albumin (1%). Only hearts with a physiological spontaneous beating rate of 500/min or higher were used for imaging to ensure consistent perfusion rates and electrical heart activity. The LV free wall was projected with the maximal cross-diameter in the objective light path for consistent imaging analysis of conduction spread. Following 10 min equilibration the heart was stained with a voltage-sensitive reporter dye (di-4-ANNEPS, Molecular Probes, Portland, OR) by injecting a 2.0 mL bolus containing 80 nmol/L into a 10 ml compliance chamber proximal to the heart aorta. When fluorescence intensity and heart rate reached steady-state, imaging was begun (typically after 8-10 mins) using an upright macro-zoom epifluorescence microscope (MVX10; Olympus) equipped with a high-speed CMOS (complementary metal oxide semiconductor) camera (Ultima-L; SciMedia), as reported previously.[4] Excitation light from a 100 W mercury arc lamp (Olympus) was passed through an interference filter (520 ± 30 nm) and a dichroic mirror (565 nm) to the heart. The emitted fluorescent light was collected with a long-pass filter (>590 nm) and projected onto the camera. The CMOS recording array was 100 x 100 pixels, and data were acquired at 2,000 frames/s with 14-bit resolution. Imaging was carried out using a 1x objective (N.A. 0.25; Olympus) at 4x zoom magnification of the left ventricular free wall.

Pacing and volumetric ECG recording

The tip of a bipolar mouse heart pacing electrode mounted on a micromanipulator device was gently positioned on the surface center of the LV free wall. Pacing capture was confirmed at 2 ms pulse length at CL 100 ms by a specialized cardiac stimulating electrode (50-100 kΩ, FHC, USA). Two custom-made Ag-AgCl electrodes were placed near the septum plane to record volume-conducted electrocardiograms (vECGs). Recordings of vECGs were amplified and low-pass filtered at 200 Hz using an electronic amplifier (HSE, Germany) and digitally sampled at 1 kHz with 16 bit resolution using the NI USB-6216 BNC (National Instruments) digitizer and custom-made software written in Labview (National Instruments). Continuous vECG recordings were obtained throughout the experiment and stored for off-line analysis. Recordings were electronically tagged to indicate the exact time of optical recording. Intermittent pacing capture was confirmed by vECG signal analysis and by optical signal analysis.

Conduction velocity measurements

The center of the LV free wall was paced at a cycle length of 100 ms by a bipolar pacing electrode (see above) to study conduction spread at a constant mouse physiological heart rate of 600 min^{-1}. All data were analyzed offline using a custom-made open source software platform written in Java and optimized for mouse heart analysis. The image sequence was filtered in space using a 5x5 uniform kernel. For each pixel, the signal was filtered in time using a moving average filter (5 frames), normalized to [0,1] and inverted. Activation time maps were obtained by measuring the activation times for each pixel. Activation times were estimated by the time (i.e. frame number) at which the fluorescence signal exceeded a given threshold (0.5). Sub-

frame accuracy was achieved by linear interpolation of the activation times. Isochrones were computed from interpolated activation time maps using a contour isochrone plot routine (Matlab, The MathWorks). The local conduction velocity was measured by two independent methods. 1) An ellipsis fitting algorithm (investigator independent) was used which approximates individual isochrones by least squares fitting and thereby determines the major (longitudinal) and minor (transversal) electrical conduction vectors from each successive isochrone within a given conduction map. The conduction maps used for ellipsis fitting were averaged from 10 consecutive cardiac cycles in order to exclude beat-to-beat variability (representative examples are shown in figure 3). Bias of the isochrone data by optical distortions due to the pacing electrode is indicated by a small symbol in each map to facilitate data review. After completion of ellipsis fitting to each thresholded and averaged data set, longitudinal and transversal isochrone data points were plotted in a distance-time graph and linearity of conduction established by linear regression. The successive data points representing a linear relation where used to determine the slope from the linear regression to estimate conduction velocity. On the other hand, data points which significantly deviated from linear behavior due to pace site proximity or organ border aberrations were excluded from the CV analysis. In addition 2) the isochrone gradient of the activation map was analyzed along the longitudinal and transversal axis as determined by the analyzing investigator. The velocity field was regularized by removing outliers, i.e. velocity vectors that deviated more than 15% in velocity or 20% in angle with respect to the corresponding average value of the nearest neighbors. Average LV conduction velocity measurements were analyzed in the major heart axis (apex to aorta) referred to as longitudinal and perpendicular referred to as transversal conduction velocity. The main vector average CV is defined as the average spatial-temporal conduction spread along the given axis and includes a homogenous data section containing conduction data within a ±15° triangle. The regions immediately surrounding the pacing electrode (a known source of stimulus CV artifact) as well as the tangentially projected heart borders or sides (a known source of ellipsoid object side border CV artifact) were excluded from the analyzed sector region used for signal analysis.

Statistical analysis

Data are represented as mean values +/- SEM except for figure 3 data which are represented as mean values +/- SD. Two-tailed Student t-test was used to compare means of two groups of samples and for more groups, an ANOVA test with a Bonferroni post-test was applied. Statistical significance was set at $P<0.05$. For conduction velocity measurements, data are represented as mean values +/- SD. In these data, t-test was applied for comparison of independent groups and $p < 0.05$ was accepted as significant.

References for the supplementary material

(1) Fanchaouy M, Polakova E, Jung C, Ogrodnik J, Shirokova N, Niggli E. Pathways of abnormal stress-induced Ca2+ influx into dystrophic mdx cardiomyocytes. *Cell Calcium*. 2009;114-21.

(2) Abi-Char J, Maguy A, Coulombe A, Balse E, Ratajczak P, Samuel JL, Nattel S, Hatem SN. Membrane cholesterol modulates Kv1.5 subunit distribution and Kv1.5-based channel function in rat cardiomyocytes. *J Physiol*. 2007;1205-17.

(3) Vaidyanathan R, Taffet SM, Vikstrom KL, Anumonwo JMB. Regulation of Cardiac Inward Rectifier Potassium Current (IK1) by Synapse-associated Protein-97. *J Biol Chem*. 2010;28000-9.

(4) Lehnart SE, Mongillo M, Bellinger A, Lindegger N, Chen BX, Hsueh W, Reiken S, Wronska A, Drew LJ, Ward CW, Lederer WJ, Kass RS, Morley G, Marks AR. Leaky Ca2+ release channel/ryanodine receptor 2 causes seizures and sudden cardiac death in mice. *J Clin Invest*. 2008;2230-45.

Online figures

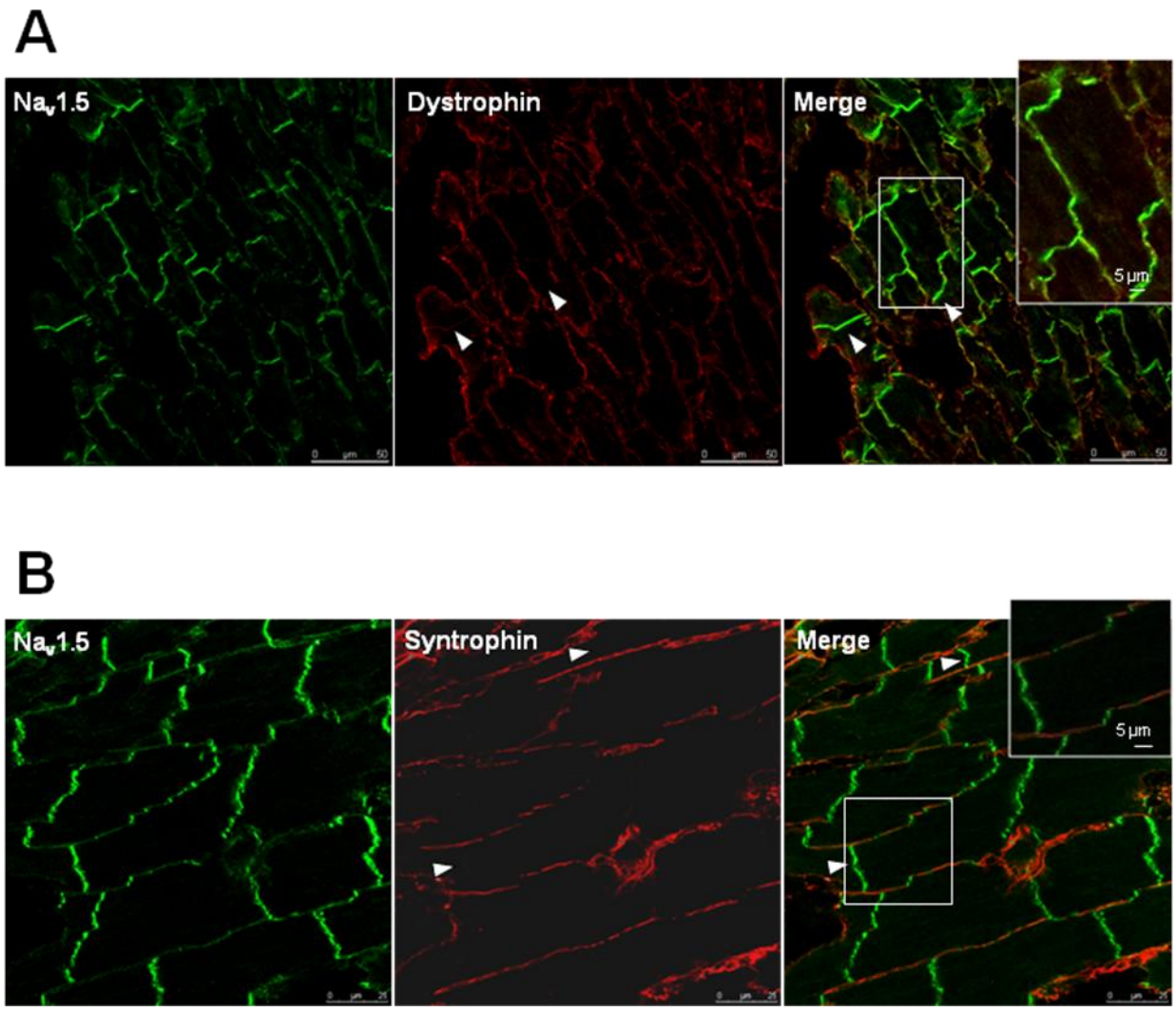

Online Fig. I. Localization of $Na_V1.5$, dystrophin and syntrophin in mouse heart ventricular sections

(A) Left: $Na_V1.5$ (green) both at the lateral membranes and the intercalated discs; middle: dystrophin (red) only at the lateral membranes; right: merge of the two images showing close localization of $Na_V1.5$ and dystrophin at the lateral membranes. The white arrow heads show the absence of dystrophin at the intercalated discs. Inset: magnification of a cell (B) Left: $Na_V1.5$ (green) both at the lateral membranes and intercalated discs; middle: syntrophin (red) only at the lateral membranes; right: merge of the two images showing close localization of $Na_V1.5$ and syntrophin at the lateral membranes. The white arrow heads show the absence of syntrophin at the intercalated discs, Inset: magnification of a portion of cell.

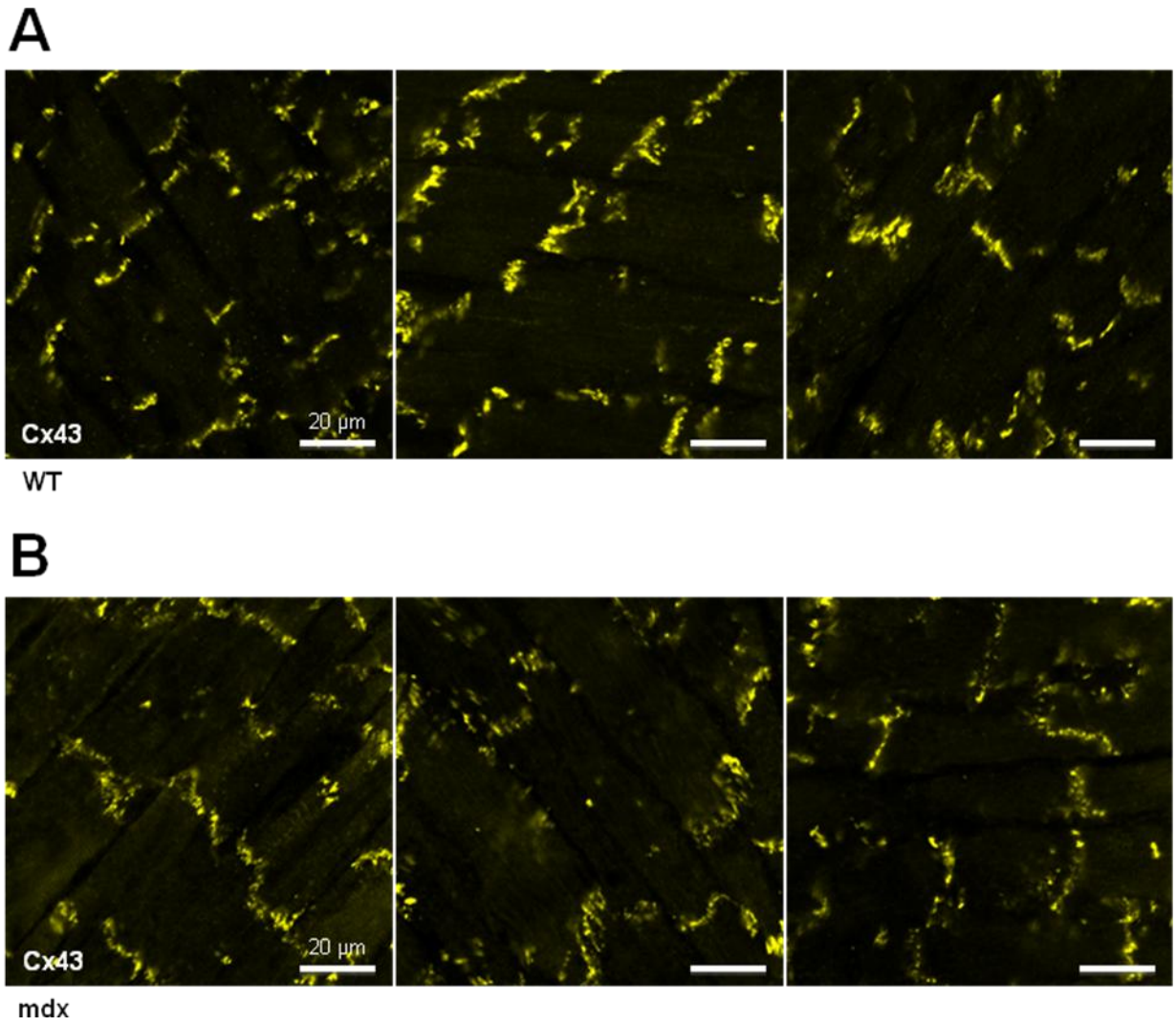

Online Fig. II. Localization of Cx43 in ventricular sections of WT and mdx mice
(A) Representative images of ventricular sections immunolabeled for Cx43 from three different WT mice, showing predominant Cx43 localization at intercalated discs of mouse cardiomyocytes. (B) In ventricular sections from mdx mice, Cx43 is similarly organized and found mainly at intercalated discs. The images are from three different mdx mouse hearts.

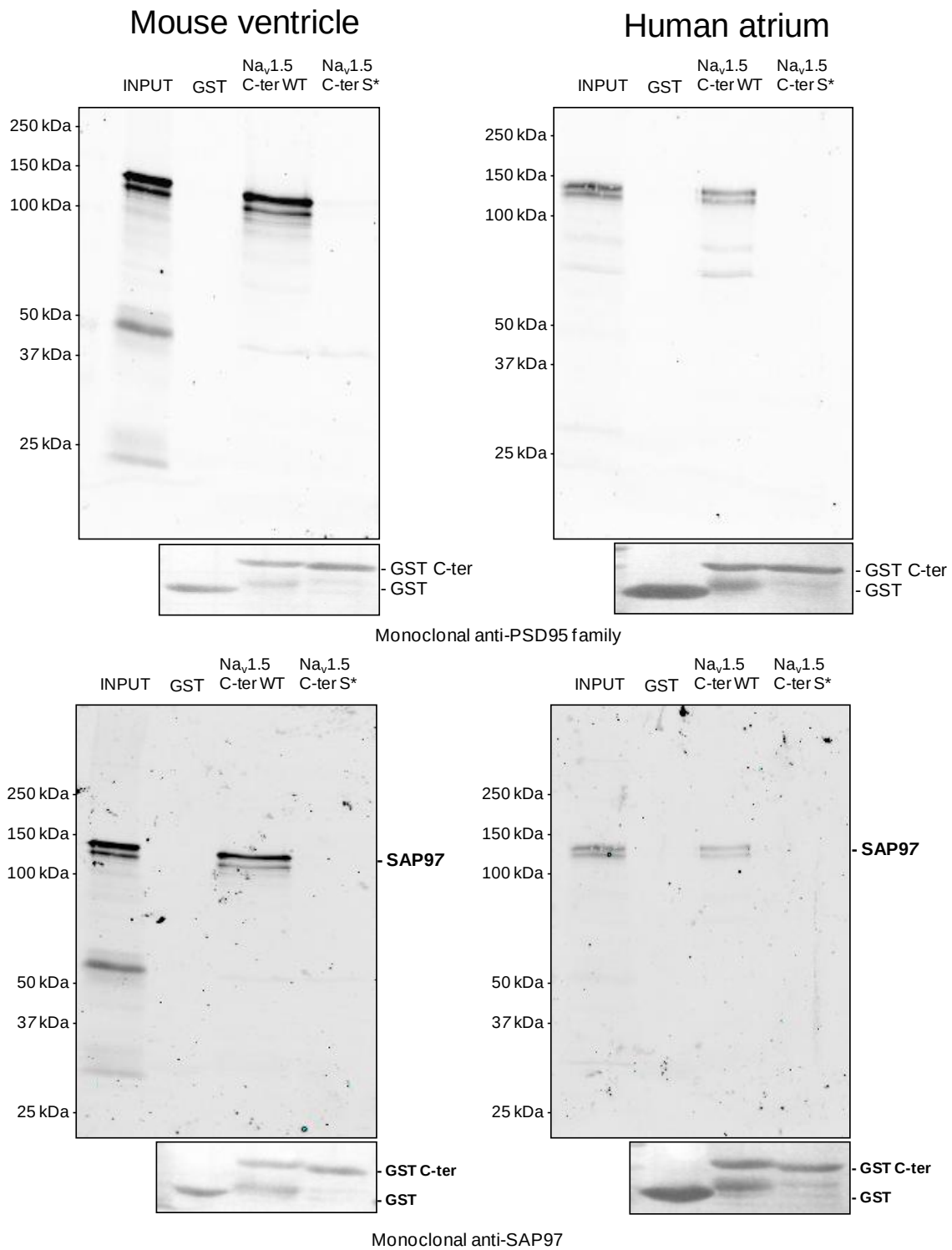

Online Fig. III.
Full size images of western blots presented in Fig. 4B and C.

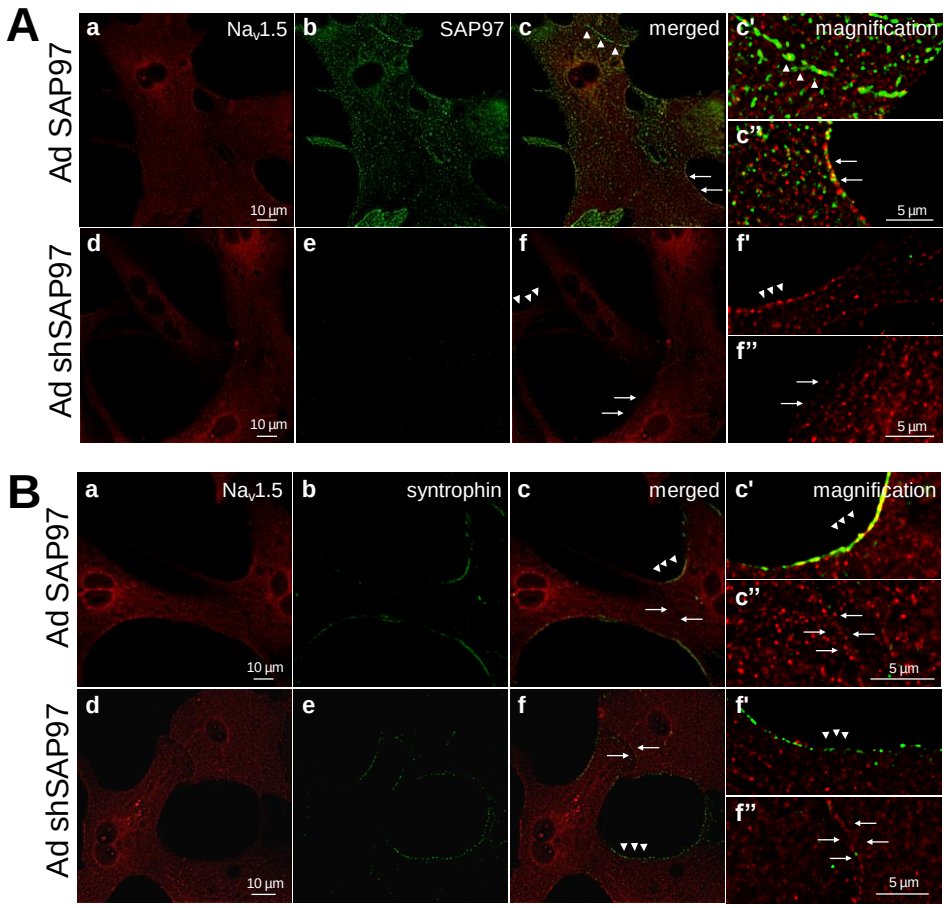

Online Fig. IV. $Na_V1.5$ co-staining with SAP97 and syntrophin in adult-cultured myocytes
(A) $Na_V1.5$ and SAP97 co-staining. **a-c**: SAP97-transduced myocytes, **d-f**: SAP97-silenced myocytes. After silencing, the expression of both SAP97 and $Na_V1.5$ channels is reduced. Note that the $Na_V1.5$ channel expression at the plasma membrane without neighboring cells (non-contact areas) is drastically inhibited. **c'** and **c''** are enlargements of two representative areas of **c** showing the high density staining for SAP97 at the level of the cell-cell contact (**c'**, arrow heads) and the expression of the SAP97 protein at a non-contact site (**c''**, arrows). **f'** and **f''** are magnifications of the SAP97-silenced myocytes in **f** illustrating the reduction of $Na_V1.5$ staining at the cell membrane.

(B) $Na_V1.5$ and syntrophin co-staining. **a-c**: SAP97-transduced myocytes, **d-f**: SAP97-silenced myocytes. The magnification image **c'** shows that some $Na_V1.5$ channels are associated with syntrophin at the level of cell border; $Na_V1.5$ staining is also observed at the level of cell-cell contacts where syntrophin staining is absent (**c''**). As in the panel A, $Na_V1.5$ channel expression is reduced after SAP97-silencing, whereas syntrophin staining remains exclusively located at non-contact areas (**f** and **f''**).

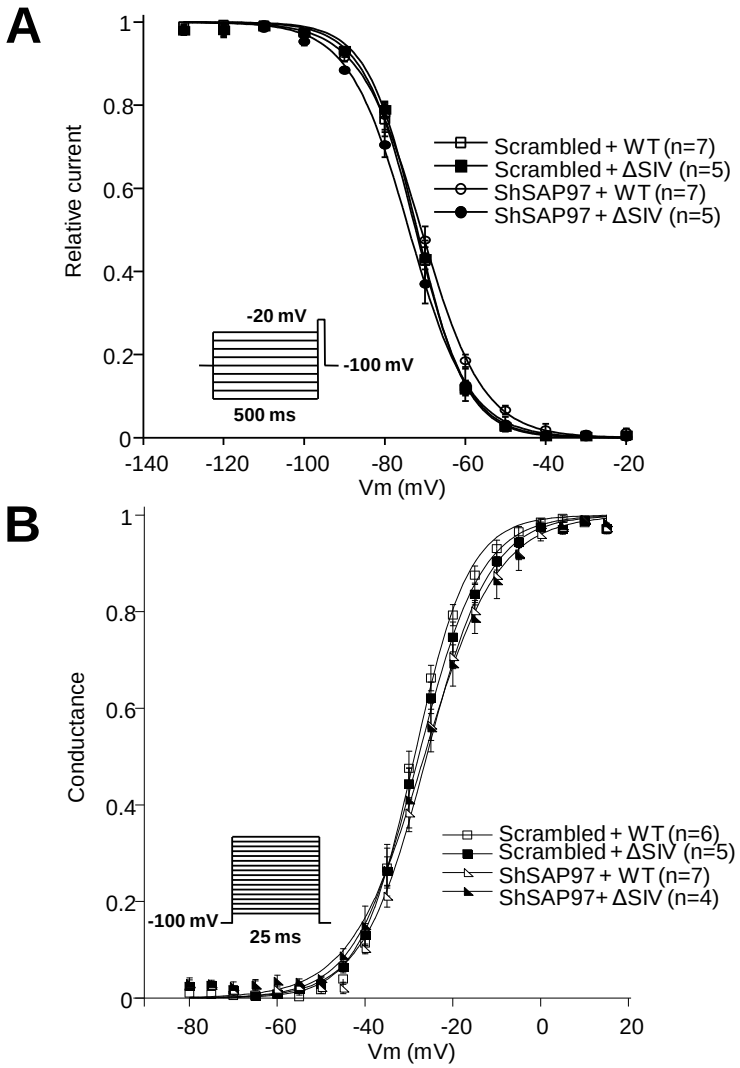

Online Fig. V. Voltage-dependence of inactivation and activation.
(A) Inactivation curves of scrambled (squares) and shSAP97 (circles) cells transiently transfected with WT (empty) or ΔSIV (black) $Na_V1.5$. Voltage-dependence of steady-state inactivation was obtained after applying a 25-ms test pulse to -20 mV after a 500-ms conditioning pulse (see inserted protocol). (B) Steady-state activation of scrambled (squares) and shSAP97 (triangles) cells transiently transfected with WT (empty) or ΔSIV (black) $Na_V1.5$. Activation properties were determined from current/voltage relationships obtained after applying the inserted step protocol. See also Material and Methods.

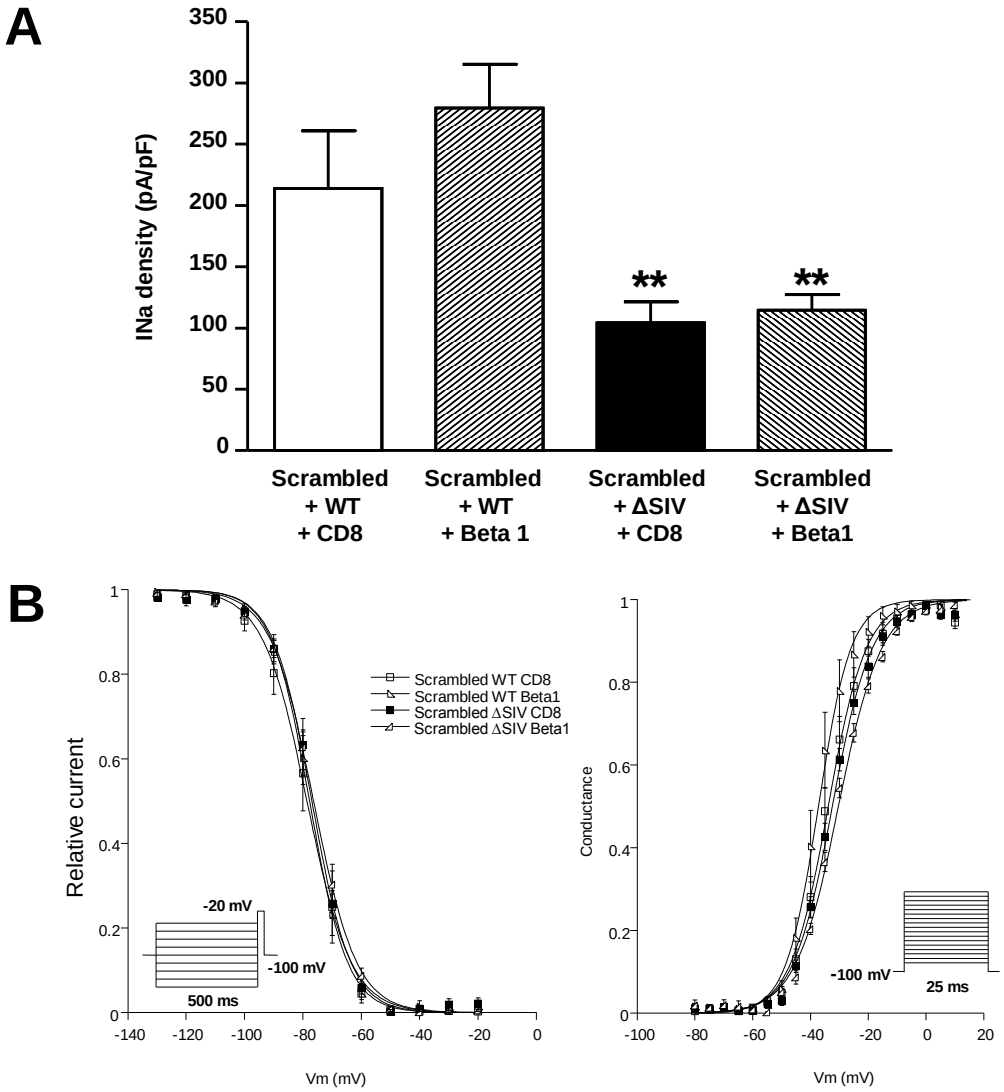

Online Fig. VI. Effect of SAP97 silencing and Beta1 on I_{Na} in HEK293 cells.

(A) I_{Na} density of scrambled HEK293 cells, transiently transfected with WT or ΔSIV $Na_V1.5$ channels with or without Beta1 subunits (CD8: reporter gene), mean values in pA/pF: Scrambled+WT+CD8: 214±62, Scrambled+WT+ Beta1: 280±42, Scrambled+ΔSIV+CD8: 104±20, Scrambled+ΔSIV+Beta1: 114±13. **p<0.01 compared to Scrambled+WT+Beta1 condition. (B) Inactivation (left) and steady-state activation (right) curves obtained after applying the inserted protocols on the corresponding cells. See also Material and Methods.

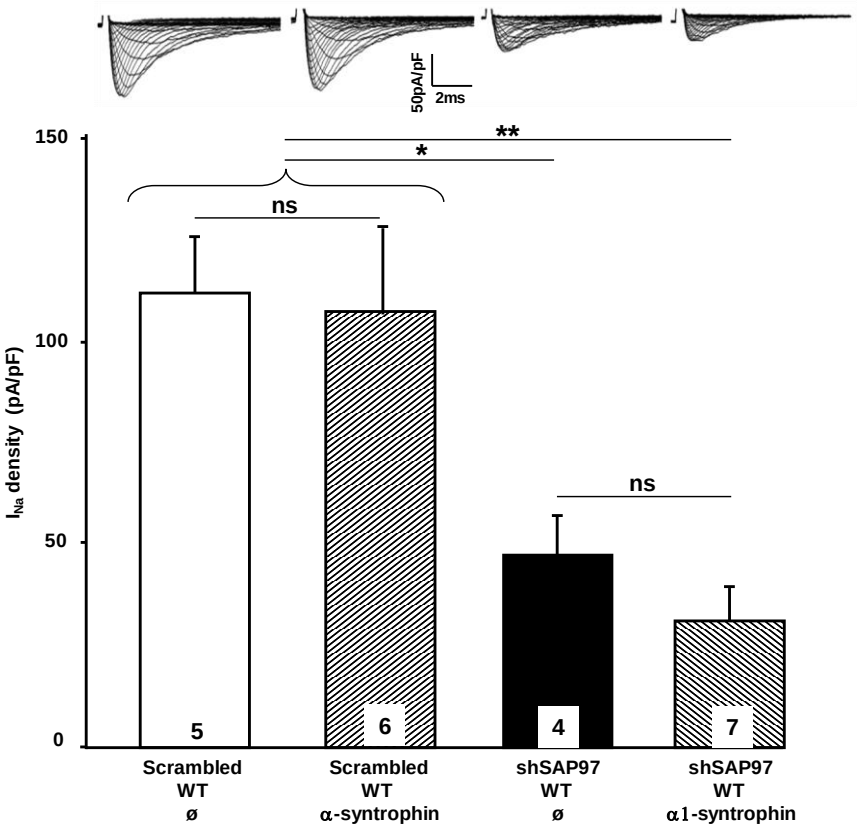

Online Fig. VII. Effect of SAP97 silencing and Syntrophin on I_{Na} in HEK293 cells.

I_{Na} density of scrambled or silenced (ShSAP97) HEK293 cells, transiently transfected with WT $Na_V1.5$ channels with or without syntrophin (inset: representative currents) (scrambled+WT+Ø: 111.9±13.7, scrambled+WT+ Syntrophin: 107.4±21.3, shSAP97+WT+Ø: 47.3±9.7, shSAP97+WT+Syntrophin: 31.35±7.9 pA/pF), *p<0.05, **p<0.01 (one way ANOVA and Bonferroni post-test). The number of cells is written in the corresponding columns.

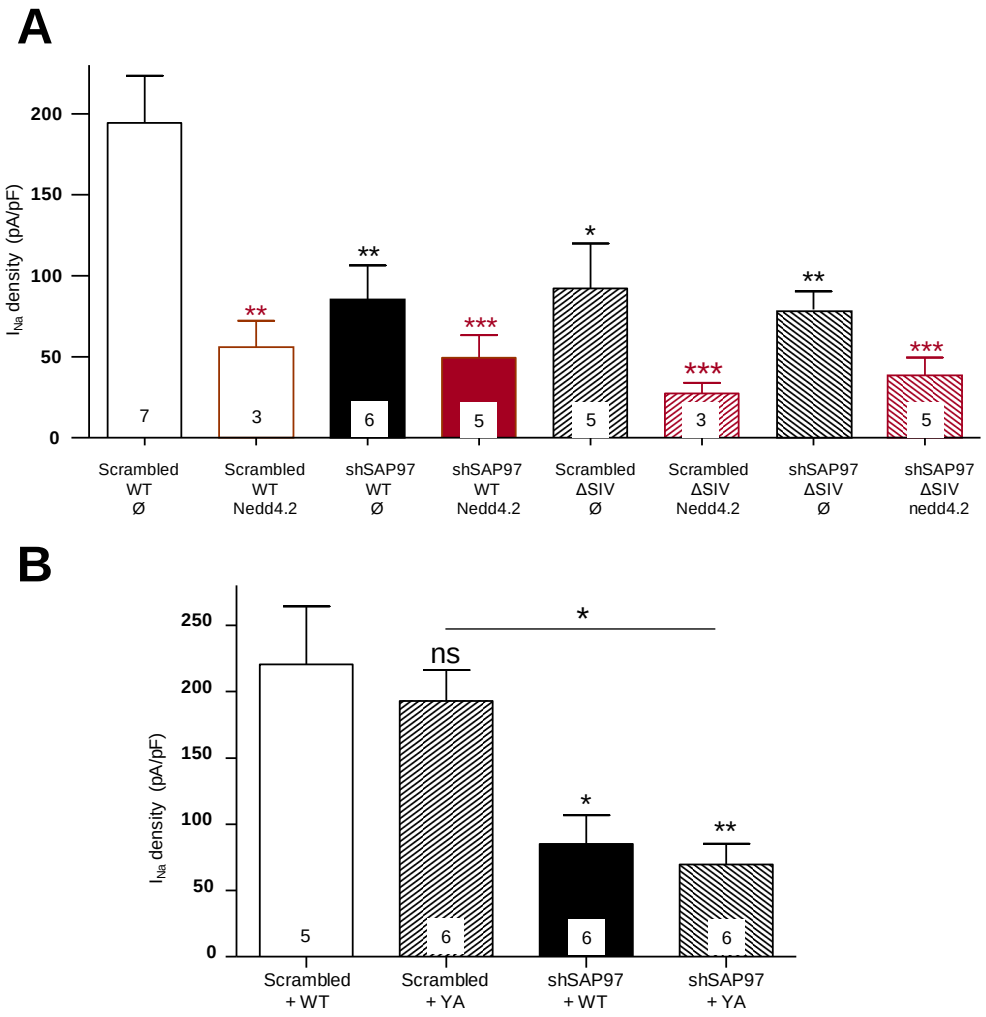

Online Fig. VIII. Investigation of the role of Nedd4-2 and PY motif of $Na_V1.5$

(A) I_{Na} density of scrambled or SAP97-silenced (shSAP97) HEK293 cells expressing $Na_V1.5$ WT or ΔSIV with empty plasmid (Ø, black columns) or Nedd4-2 (red columns), *p<0.05, **p<0.01, ***p<0.001 (one way ANOVA and Bonferroni post-test, compared to the "scrambled + WT + Ø" condition). (B) I_{Na} density of scrambled or silenced (ShSAP97) HEK293 cells, transiently transfected with $Na_V1.5$ WT or YA *p<0.05, **p<0.01; ns: not significant (one way ANOVA and Bonferroni post-test compared to the "scrambled + WT" condition). Number of cells is written in the corresponding columns.

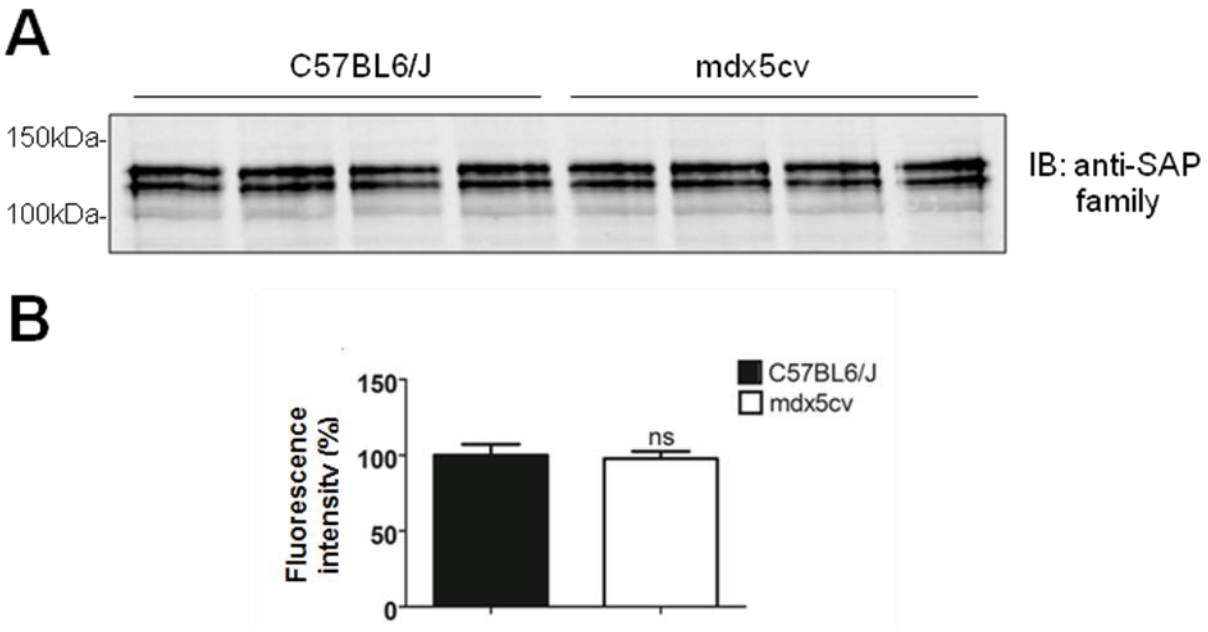

Online Fig. IX. SAP97 protein level is comparable in hearts of mdx5cv mice compared to WT.

For comparison of the amounts of SAP97 present in the hearts of control and mdx5cv mice, 40 µg of ventricular lysates were loaded on SDS-page gels. The protein concentration of each lysate was measured in triplicate by Bradford assays to guarantee equivalent loading and confirmed by Ponceau coloration. (A) Representative Western blots performed with the indicated antibodies. (B) The amount of SAP97 examined in four hearts for each genotype was assessed by fluorescence intensity quantification with LICOR Odyssey software. Statistical significance was tested with a two-tailed Student's t-test.